

FURTHER STUDIES
ON
VIBRATION COMPACTION
OF
COHESIVE SOILS

CALIFORNIA INSTITUTE OF TECHNOLOGY

September 1955

FURTHER STUDIES
ON
VIBRATION COMPACTION
OF
COHESIVE SOILS

A continuation of the research
into the basic laws
governing compaction of soil
by oscillating surface loads

A research project sponsored by
U. S. Navy Bureau of Yards and Docks,
U. S. Naval Civil Engineering and Research Laboratory
Port Hueneme, California

CALIFORNIA INSTITUTE OF TECHNOLOGY
September 1955

PREFACE

Object

The investigations described in this report are a continuation of previous work designed to determine the basic laws governing the compaction of cohesive soil by vibration. A report dated December, 1954, described the results of tests on sandy loam, while this report describes similar tests on a much more cohesive soil.

Authority

The present investigation was sponsored by the U. S. Navy Bureau of Yards and Docks, U. S. Naval Civil Engineering Research and Evaluation Laboratory, Construction Battalion Center, Port Hueneme, California, under an extension of Contract NOy-22271.

Personnel

Supervision of the Project for the Navy was under the direction of Mr. John A. Bishop, Head of the Soils and Pavement Division, NAVCERELAB, Port Hueneme, and Mr. Charles R. White, his assistant.

The California Institute of Technology staff consisted of Professor Frederick J. Converse, Project Director; Mr. William F. Jones, Project Engineer; Professors George W. Housner and Donald E. Hudson, Consultants; and Mr. David M. Wilson and Mr. Rudolf E. Ribbens, Assistants.

Synopsis

Previous reports on the Project work have been issued under the dates of March 1950, "An Investigation of the Compaction of Soil by Vibration"; January 1952, "Vibration-Compaction of Sand"; and December 1954, "Vibration Compaction of Cohesive Soils." The investigations since the publication of the last report have consisted mainly of field tests with a small oscillator on prepared soil, and a small amount of laboratory

work to determine the physical characteristics of the soil--its shearing strength and its modulus of rigidity under varying density and moisture conditions.

For the field tests, the prepared soil was placed in a pit excavated in the natural soil. Controllable vertical oscillating forces were supplied by Lazan oscillators consisting of rotating eccentric weights mounted on contra-rotating shafts and driven by a flexible shaft from a Varidrive motor. Sometimes one oscillator, and at other times an assembly of two oscillators in series, was used. Weights were added as necessary to get the required unit soil pressures on areas varying from $1/2$ to $1-1/2$ square feet.

Previous investigations had indicated that the most rapid compaction occurs when the oscillator-soil system is vibrating at the resonant frequency. For cohesive soil, the term "resonant tamping" is perhaps more descriptive of the actual process of compaction than "resonant vibration," since the major requirement is the development of sufficient force to cause shearing failure within the soil. In these tests, studies were confined to the effect of the following parameters on the density of the soil when the oscillator-soil was at resonance for a definite period of time. The variables were:

- (i) Moisture content of the soil;
- (ii) Unit soil pressure;
- (iii) Size of the base plate;
- (iv) Ratio of applied dynamic force to dead weight of the oscillator.

Conclusions from the tests on the more cohesive soil (following the work on the sandy loam) must be considered as tentative. The reason for this is attributed to the low dynamic force, inherent in the available oscillators, at the resonant frequencies occurring in these tests, thereby rendering it impossible to cover the entire range of the variables being investigated. The conclusions are that good densities of cohesive soils can be obtained by vibration-compaction, providing (a) the oscillator is operated at resonant frequency; (b) the ratio of applied dynamic force to dead weight is approximately unity; (c) the unit soil pressure due to the dead weight of the oscillator is at least 8 pounds per square inch (for the soil tested); and (d) the moisture content is as high as practicable for the density required. Best results were found to occur when the moisture was on the wet

side of the optimum value given by a laboratory moisture-density curve (modified A.A.S.H.O.).

Summing up the experience with the three types of soil studied under this contract and its extensions, the following general conclusions may be drawn:

1. Vibration at resonance of the vibrator-soil system is of major importance in getting rapid consolidation.
2. A ratio of applied dynamic force to dead weight of the vibrator approximately equal to unity is desirable for maximum effectiveness.
3. For dry cohesionless sand, only very low unit soil pressures are required. A pressure as low as 3 psi gave excellent results.
4. Increasing moisture in sand up to a certain limiting value (about 8% for the sand used in the tests) develops cohesion in the sand, and requires greater unit soil pressure in order to develop equal density than is required for dry sand.
5. The more cohesive the soil, the higher is the unit contact pressure necessary for compaction. In the sandy-loam soil described in the report of December 1954, dead weight pressures of 4 psi were used successfully, while for the clay loam soil of the present program dead weight pressures of 8 to 10 psi were required.
6. It is desirable to use as high a moisture content of clayey soils as is commensurate with density requirements, since the magnitude of the cohesion is a measure of the pressure required for compaction and since the cohesion of clayey soils decreases with increase in moisture content. The value of the moisture content appears to be slightly greater for the same maximum density than the optimum moisture content found by the modified A.A.S.H.O. compaction method.
7. The addition of certain chemicals, such as sodium sulphate and Daxad-23, to the soil, tends to reduce the cohesion and therefore decreases the effort necessary to compact the soil.

TABLE OF CONTENTS

	Page
PREFACE	(iii)
NOTATION	(xiii)
ERRATA IN "VIBRATION COMPACTION OF COHESIVE SOILS"	(xv)
CHAPTER 1 - FIELD INVESTIGATIONS	1
1.1 Object	1
1.2 Scope	1
1.3 Type of Soil	1
1.4 Planning	2
1.5 Preparation of Test Area	4
1.6 Test Program	6
1.6.1 Equipment	6
1.6.2 Procedure	14
1.6.3 Density Measurements	15
1.6.4 "Spread" of Compactive Effect	16
1.7 Contact Pressure and the Necessity to Operate at Resonance	16
1.7.1 Theoretical Considerations	19
1.8 Measurement of Contact Pressures	20
1.9 Calculation of Contact Pressures	20
1.9.1 Linear and Non-Linear Vibrating Systems	20
1.9.2 Displacement Analysis Method for Calculating Contact Pressures	23
1.9.3 Phase-Angle Analysis Method for Calculating Contact Pressures	26
1.10 Test Results	37
1.10.1 Effect of the Soil Moisture Content	38
1.10.2 Effect of the F_0/W Ratio	43
1.10.3 Effect of the Dead Weight, Dynamic Force, and Contact Pressure	42

TABLE OF CONTENTS - (Continued)

	Page
1.10.4 Effect of the Diameter of the Base Plate	50
1.10.5 Effect of Movement of the Vibrator over the Soil Surface	53
1.11 A Practical Comparison of the Methods of Displacement and Phase-Angle Analysis	53
References	60
CHAPTER 2 - LABORATORY INVESTIGATIONS	61
2.1 Introduction	61
2.2 Shearing Resistance of Compacted CL Soil	61
2.2.1 Material	61
2.2.2 Equipment	61
2.2.3 Procedure	62
2.2.4 Results	62
2.3 Tests for Modulus of Elasticity in Shear	64
2.3.1 General	64
2.3.2 Apparatus	64
2.3.3 Procedure	66
2.3.4 Test Results	66
2.3.5 Conclusions	70
References	70
CHAPTER 3 - SUMMARY AND CONCLUSIONS	71
3.1 Discussion and Summary	71
3.2 Conclusions	72
3.3 Recommendations for Future Studies	73

List of Tables

Table No.		Page
1.1	Summary of Data from Tests with Lazan Oscillators	7
1.2	Planned Conditions for Tests with Lazan Oscillators	10
1.3	Data from Experiments by Pauw	18
1.4	Basic Data from Test L11-47	24
1.5	Calculation of Dynamic Amplification Factors - Test L11-47. Displacement Analysis Method	27
1.6	Calculation of Phase Angles, Test L11-46	36
1.7	Tests Conducted to Investigate Moisture-Density Relationship	40
1.8	Total Vibrating Mass in Tests L11-42 to L11-47	45
1.9	Dynamic Amplification Factors and Contact Pressures for Resonant Conditions in Tests L11-42 to L11-47. Displacement Analysis Method	48
1.10	Tests to Determine Effect of Size of Base Plate on Density of Soil	52
1.11	Dynamic Amplification Factors and Contact Pressures for Resonant Conditions in Tests L11-45 to L11-47. Phase-Angle Analysis Method	55
2.1	Summary of Direct Shear Test Results	63
2.2	Summary of Results from Torsion Tests on Unconfined Cylinders	67

List of Figures

Figure No.		
1.1	Particle Size Distribution Curve for Reseda CL Soil	3
1.2	Relation between Moisture Content and Dry Density obtained with the Reseda CL Soil when Compacted by the Modified A.A.S.H.O. Method	3
1.3	Distribution of Stresses under a Loaded Circular Area	21
1.4	Relationship between Frequency Ratio and Amplitude Ratio. Comparison between Theoretical Curves for a Linear System with various Damping Factor Ratios and the Test Curve from Test L11-47	25

List of Figures - (Continued)

Figure No.		Page
1.5	Relationship between Frequency and Normalised Amplitude, Test L11-47	28
1.6	Relationship between Frequency and Normalised Amplitude, Test L11-45	28
1.7	Increase in Dynamic Force with Increase in Frequency, Test L11-47	29
1.8	Relationship between Frequency Ratio and Normalised Amplitude, Test L11-47	29
1.9	Relationship between Frequency Ratio and Phase-Angle for a Linear Vibrating System with various Damping Factor Ratios	31
1.10	Basic Diagrams used to Set-up Phase-Angle Analysis Equations	35
1.11	Relationship between Frequency of Vibration and Phase Angle between Applied Dynamic Force and Vibrator Motion, Test L11-46	39
1.12	Relationship between Frequency Ratio and Phase Angle, Test L11-46	39
1.13	Moisture-Density Relationships in Tests L11	41
1.14	Increase in Dynamic Amplification Factor with increase in F_o/W Ratio, from tests by Pauw	41
1.15	Relationship between Nominal Contact Pressure and Maximum Recorded Dry Density for a Moisture Content of 16% to 17%, and Base Area of 148 Sq. In., Tests L11	47
1.16	Relationship between Nominal Contact Pressure and Maximum Recorded Dry Density for a Moisture Content of 20%, and a Base Area of 74 Sq. In., Tests L11	47
1.17	Relationship between Nominal Contact Pressure and Maximum Recorded Dry Density for a Moisture Content of 20% and a Base Area of 148 Sq. In., Tests L11	47
1.18	Relationship between Base-Plate Diameter and Maximum Dry Density, Tests L11	51
1.19	Slip Lines for a Load acting on the Edge of a Metal Plate, from "Plasticity" by A. Nadai.	51

List of Figures - (Continued)

Figure No.		Page
1.20 to 1.23	Effect of Frequency of Vibration on Dynamic Amplification Factor and Dynamic Contact Pressure in Tests L11-42 and L11-43, as Determined by the Displacement Analysis Method	56
1.24 to 1.27	Effect of Frequency of Vibration on Dynamic Amplification Factor and Dynamic Contact Pressure in Tests L11-44 and L11-44A, as Determined by the Displacement Analysis Method	57
1.28 to 1.31	Effect of Frequency of Vibration on Dynamic Amplification Factor and Dynamic Contact Pressure in Tests L11-45 and L11-46, as Determined by the Methods of Displacement Analysis and Phase-Angle Analysis	58
1.32 to 1.33	Effect of Frequency of Vibration on Dynamic Amplification Factor and Dynamic Contact Pressure in Test L11-47, as Determined by the Methods of Displacement Analysis and Phase-Angle Analysis	59
2.1	Relationship between Moisture Content and Cohesion, Angle of Internal Friction, and Shear Strength of Reseda CL Soil	65
2.2	Apparatus used in the Experimental Determination of the Shearing Modulus of Elasticity of Reseda CL Soil	65
2.3	Relationship between Moisture Content and Shearing Modulus of Elasticity of Reseda CL Soil, showing Effect of Varying the Normal Load	68

List of Plates

Plate No.		Facing Page
1.1	Equipment Assembly using One Lazan Oscillator, with Electrical Instruments to Measure Frequency and Displacement	14
1.2	(A) Equipment Assembly using Two Lazan Oscillators geared together. The Impulse Pick-Up is mounted on the bracked covering the Top of the Upper Gear Wheel	15

List of Plates - (Continued)

Plate No.		Facing Page
1.2	(B) Equipment Assembly using Two Lazan Oscillators geared together. The Dials showing Angular Eccentricity and the Knurled Control Knobs can be seen. Two Velocity Pick-Ups are Mounted on the Top Dead Weight Plate	15
1.3	A Portion of the Miller-Oscillograph Chart for the Resonant Condition in Test L11-46	32
1.4	(A) Assembly of Brush Instruments in early Attempts to Measure Phase-Angles (B) Assembly of Miller Instruments in later Attempts to Measure Phase-Angles	33
2.1	Apparatus for the Determination of the Shearing Modulus of Elasticity of Reseda CL Soil, using Dial Gages to Measure Angle of Twist	68
2.2	Apparatus for the Determination of the Shearing Modulus of Elasticity of Reseda CL, using Optical Methods to Measure Angle of Twist	69

NOTATIONS

A	area of base-plate of vibrator
c	(1) damping factor ratio, β/β_c (2) unit soil cohesion
F_o	applied dynamic force resulting from rotation of the eccentric weights in the Lazan oscillators
\bar{F}	calculated effective dynamic force
\bar{T}	calculated effective unit dynamic contact pressure between base-plate and soil surface
f_1	applied dynamic contact pressure, Pauw
f_2	measured dynamic contact pressure, Pauw
G	shearing modulus of elasticity
I	polar moment of inertia
k	spring factor of the soil
L	(1) wave length measured on oscillograph chart (2) length of torsion specimen
l	lag distance of velocity pick-up wave as measured on oscillograph chart
M	applied torque
m_t	total mass of vibrator-soil system
m_v	mass of vibrator
N	normal load in plane of maximum shear
n	subscript indicating a value at resonant frequency
R	rate of travel of oscillograph chart
s	shear strength of the soil
T	theoretical maximum allowable torque before end slippage in torsion tests
W	dead weight of vibrator
w	soil moisture content

NOTATIONS - (Concluded)

β	damping factor of vibrator-soil system
β_c	critical damping factor of vibrator-soil system
δ	amplitude of vibration
θ	angular setting of Lazan oscillator eccentric weights
σ_1	vertical pressure
σ_3	horizontal pressure
ϕ	(1) phase angle between applied dynamic force and motion of vibrator (2) angle of internal friction of soil (3) total angle of twist in length L of torsion specimen
ϕ_1	apparent phase-angle
ϕ_2	phase-angle correction
ω	frequency of vibration
ω_n	resonant frequency

ERRATA
IN REPORT OF DECEMBER 1954
"VIBRATION COMPACTION OF COHESIVE SOILS"

- p. (ix)* Chapter 5 is "SUMMARY AND CONCLUSIONS."
- p. (xi) description for Figure 3.2 should show Daxad 23.
- p. 6 the heading for column (5) should be $\frac{(F + W)}{A}$.
- p. 8 the third last line in section 1.6.1 should read as follows:
". . . in Appendix C on plates"
- Facing Plate 2.2, the two photographs should be exchanged in position, caption (A)
p. 25 referring to the present lower photograph and caption (B) referring to the
present upper photograph.
- p. 29 Fig. 2.10, change L1, L2, L3 to L8, L9, L10.
- p. 32 Fig. 2.12, change the range of the Frequency axis from "8 to 28 c.p.s." to "6.8 to 18.8 c.p.s."
- p. 37 Fig. 2.18, change the legend to show the solid block circles indicating the moisture content range 11.0% to 13.7%, and the open circles indicating the moisture content range 7.9% to 9.9%.
- p. 40 change the equation at the bottom of the page to read:
$$\gamma_d = 74.2 + 36.2 p^{-0.655}.$$
- Facing change "of" to "by" in the caption under the photograph
p. 40
- p. 42 change the equation at the top of the page to read:
$$\gamma_d = 74.9 + 34.6 p^{-0.589}.$$
- p. 85 section 4.4.2, line 3, change "stories" to "stones."

* Page numbers refer to pages in the report dated December 1954.

(concluded next page)

ERRATA - (Concluded)

- p. 85 section 4.4.2, line 6, change "to shear" to "in shear."
- p. 88 line 8, change "vibrations" to "variations."
- p. 88 section 4.4.4, line 1, insert "aspect" after "significant."
- p. 109 change equation (5.29) and the following relationship to read:

$$E = E'(h+z)$$

$$\text{where } E' = \frac{dE}{dz} \quad \text{a constant for a given soil}$$

- p. 109 last paragraph, line 2 should read as follows:
". . . have finite values at the soil surface even when the soils are
not under load. That is, $E \dots$ "
- p. 109 last paragraph, line 3, omit the word "even."

ERRATA
IN REPORT OF SEPTEMBER 1955
"FURTHER STUDIES ON VIBRATION COMPACTION
ON COHESIVE SOILS"

- p. (vii) page number for section 1.7.1 should be 18.
- p. (ix) page number for table 1.3 should be 17.
- p. 1 second line in section 1.3 should read as follows:
 "A supply of a clayey-silt, containing a good percentage of sand sizes".
- p. 2 line 19, change "5.9%" to 8.6%".
- p. 30 line 8, change "this" to "the".
- Facing
p. 32 Plate 1.3, add an arrow pointing to the left alongside "Movement of Chart".
- p. 38 in heading for section 1.10.1, delete "and".
- p. 42 last paragraph, line 6, insert a comma after "was".
- p. 46 last line of text, delete "of".
- p. 52 first paragraph after Table 1.10, line 5, insert "a" between "and" and
 "similar".
- p. 55 line 12, add "method" after "analysis".
- Facing
p. 68 Plate 2.1, omit prefix (A) from caption.
- Facing
p. 69 Plate 2.2, omit prefix (B) from caption.

CHAPTER 1

FIELD INVESTIGATIONS

1.1 Object

The majority of the tests described in the following text formed a continuation of earlier work, designed to provide basic resonance and compaction data from which optimum field operating conditions for the compaction of cohesive soils by vibration may be determined.

1.2 Scope

Assuming the previously established principle that maximum compaction occurs at resonance, the effect of each of the following variables on density and resonant frequency was investigated, within certain previously delineated limits:

- (1) Soil moisture content - w ;
- (2) Ratio of dynamic force to dead weight - F_o/W ;
- (3) Dead weight of the vibrator - W ;
- (4) Dynamic force of the vibrator - F_o ;
- (5) Contact pressure between the base of the vibrator and the soil surface;
- (6) Diameter of the base-plate of the vibrator;
- (7) Movement of the vibrator over the surface of the soil.

1.3 Type of Soil

A highly cohesive soil was desired in order to supplement previous work on moderately cohesive soil. A supply of a sandy silt, containing a good percentage of clay sizes was obtained. This material was classified as Clay Loam by the U. S. Bureau of Soils Trilinear classification, and as CL-type soil by the modified Casagrande airfield classification. A curve of particle-size distribution is shown in Fig. 1.1; and additional

data are tabulated below.

Liquid Limit	-	39	
Plasticity Index	-	21	
Specific Gravity	-	2.67	
Particle-size distribution, %:		M.I.T.	U.S.B.S.
Sand	-	24	29
Silt	-	61	44
Clay	-	15	27

Classification (modified Casagrande):

CL-type; inorganic clayey-silt of medium plasticity.

The moisture-density relationship of the soil was determined by the modified A.A.S.H.O. method as used by the U. S. Navy, i.e. 25 blows of a 10 lb. hammer falling freely 18 in. each blow, on each of 5 lifts of soil contained in a cylindrical mould 1/30 cu. ft. in volume. The relationship is shown in Fig. 1.2, the important values used as control throughout the field test being:

Maximum dry density	-	112.8 lb./cu.ft.
Optimum moisture content	-	14.6%
90% of maximum dry density	-	101.5 lb./cu.ft.
Air voids at max. density	-	5.9%

Throughout the text this soil is described as Reseda CL soil, having been obtained from the Reseda area of the San Fernando Valley in Southern California.

1.4 Planning

At the outset of this work, a fairly comprehensive programme of operations was drawn up in which the tests, to be conducted in the pit in the natural ground at the California Institute of Technology, were arranged in a logical, but flexible, manner. The flexibility was considered very necessary due to the uncertainty concerning the amount of time that would be consumed in conducting a test from the commencement of filling the pit to the final emptying after the test. It was planned to investigate fully the effects

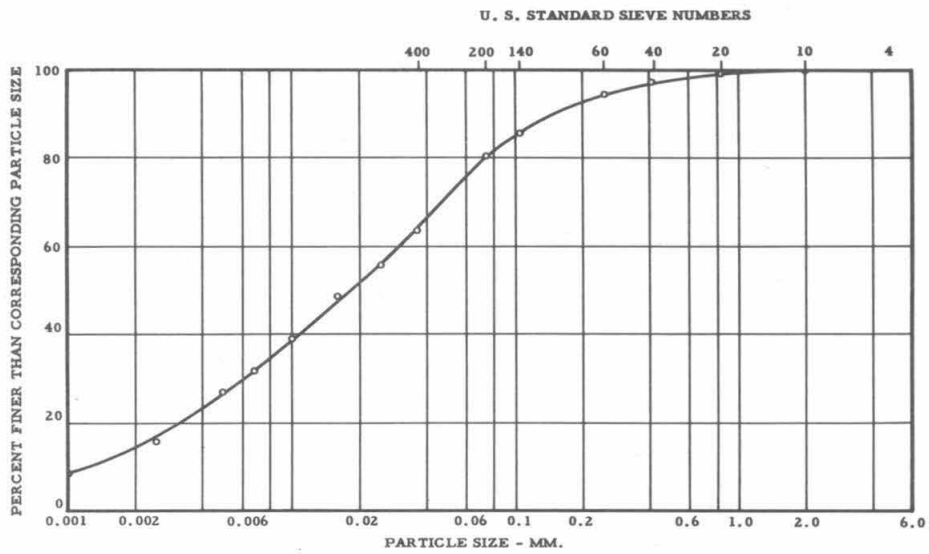


Fig. 1.1 PARTICLE SIZE DISTRIBUTION CURVE FOR RESEDA CL SOIL

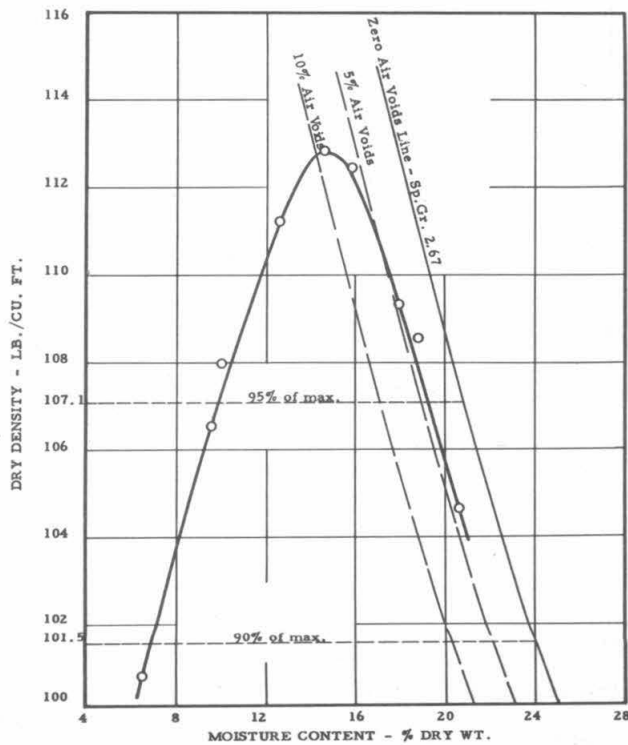


Fig. 1.2 RELATION BETWEEN MOISTURE CONTENT AND DRY DENSITY
OBTAINED WITH THE RESEDA CL SOIL WHEN COMPACTED
BY THE MODIFIED A.A.S.H.O. METHOD

of all of the parameters outlined in section 1.2 of this chapter, except numbers (6) and (7), at a given moisture content, then to adjust the moisture content and investigate the effects of the other parameters at this new moisture value, continuing in this manner until a sufficient range of moisture content had been covered. It was realized at the outset that the complete list of parameters could not all be fully investigated with the funds available, hence (6) and (7) were only to be considered at one particular moisture content when and if the time was available and the opportunity was presented.

1.5 Preparation of Test Area

The tests were all conducted in the pit in the natural ground at the California Institute of Technology. This pit was the one used in previous work on sandy loam described in the Report to the U. S. Navy dated December 1954. It measured 3 feet deep by 4 feet wide by 8 feet long, with end slopes 3 feet long from the ground surface to the bottom of the pit, to facilitate rolling of the test soil during placing. A cushion of loosely compacted soil was placed in the bottom of the pit, reducing its depth to between 2 feet and 2 feet 6 inches. Measurements in the surrounding natural soil indicated that its density was about 80% of maximum, and by periodic application of moisture, the moisture content of this soil was maintained at approximately 10%, except within an inch or two of the ground surface. During the initial excavation of the pit, the whole area had been extensively disturbed so that the hard cemented nature of the natural fine-grained soil at this location had been destroyed, the pit being formed by filling and compacting the surrounding soil behind formwork. The periodic application of moisture was felt sufficient to prevent the reappearance of undue hardness due to drying out, this being confirmed by a number of penetration tests using a Proctor Needle, and by the ease with which lumps of soil taken from below the surface could be broken in the hand.

Various methods of breaking-up, mixing, and laying the test soil were tried in an attempt to give, as far as was practicable, a homogeneous mass from the point of view of density and moisture content. Cement or plaster mixers proved completely unsuitable due to the cohesiveness of the soil, and with the resources available to the Project, only one method proved successful. This entailed weight-batching soil containing about 100 pounds of dry particles, adding an amount of water based on numer-

ous control moisture determinations of the soil in the storage bins, rough shovel-mixing the soil in the batching trays, sieving the soil by raking over a large sieve, spreading the sieved soil by raking, and rolling this soil using a small hand roller. After numerous trials, and taking into consideration the time element involved in the sieving process, a wire mesh was obtained having a square opening of 4.75 mm., a wire diameter of 1.60 mm., and a percentage open area of 56.0. This closely approximates the dimensions of a U. S. Standard Sieve No. 4. The sieve used in the preparation process consisted of a piece of this wire cloth 2 feet by 3 feet, supported on 3/8-inch diameter steel bars at 6 inch centers firmly screwed into boards along the long edges of the cloth.

The sieve was supported on beams layed across the pit, and about 300 pounds of soil was sieved at each of a number of adjacent points along the pit. The resulting pyramids of soil were then raked and levelled, and rolled to give a layer thickness of about 3 inches. It was found that the roller compacted the soil to refusal after about 5 passes, and that a density of about 67% of maximum could be obtained this way. A density of about 63% of maximum was obtained with 4 inch to 5 inch lifts, but the higher density with its attendant probability of greater uniformity was preferred. Towards the end of the program, the pit was filled at a density of almost 80% of maximum to investigate the effect of the initial density on the final density after vibration. No appreciable difference in final density was found between the tests with initial densities of 67% and 80% of maximum, that could be attributed to the difference in these initial densities.

Preparation of the test area in the manner detailed here was unfortunately slow for this cohesive soil, and depended greatly upon the amount of additional water required when raising the moisture content from a low value to a higher one. Where water was required only to maintain a particular soil moisture content, the time taken to fill the pit, run the tests, take density measurements, and empty the pit, was about 7 to 8 working days. When water had to be added to raise the soil moisture content by the normal increment of 2%, e.g. from 14% to 16%, the time for the complete test cycle increased to 9 and 10 working days. When no moisture at all had to be added to the soil, the test cycle was easily reduced to 4 or 5 working days.

1.6 Test Program

In all, some fifty-two tests were conducted at the California Institute of Technology pit. Identification of these tests followed directly the identification of the series of earlier tests on sandy loam, which had been denoted by the prefixes L1, L2, L3, L9, L10. Since a change in the prefix number was made only when the properties of the soil being tested were significantly altered, as by adding chemicals to the soil or by taking a new soil altogether, the present series were all prefixed by the number L11, and were numbered consecutively L11-1, L11-2, L11-3, etc., in chronological order. The suffix A, such as in L11-3A, was used to denote a test run under identical conditions to an earlier test of the same basic number which, in the case of the example given, was test L11-3.

A summary of the important data from the tests is shown in Table 1.1. All values of dynamic force (F_o) shown in the table are the values occurring at resonant frequency. The soil moisture contents are the average values in the upper 12 inches of soil in the pit immediately after the test, and are shown as "class values" in all cases. That is, if the moisture content shown in the Table is w , then the exact test value lies within the range $w \pm 0.5\%$, w then being the "class value."

Since the actual conditions obtained in a test did not always conform to the conditions planned before the test, Table 1.2 is presented to afford comparison with the values actually obtained. Thus, Table 1.2 shows that in Tests L11-23, L11-24, L11-25, it was desired to obtain values of the F_o/W ratio of 0.8, 1.20, and 2.00 respectively, and settings of the machine were adjusted accordingly. However, resonant frequency was such that the actual values of the F_o/W ratio were respectively 0.85, 1.00, and 1.03.

1.6.1 Equipment

The equipment used to conduct the tests with was the same as that used in the previous vibration work with less cohesive soils. Essentially it consisted of a Lazan oscillator driven by a 1 H.P. 110-volt A.C. single-phase motor equipped with a Vari-drive and flexible shaft transmission. The motor itself ran at constant speed, variation in speed being given to the flexible shaft by the belt and pulley arrangement of the Vari-

TABLE 1.1

SUMMARY OF DATA FROM TESTS WITH LAZAN OSCILLATORS

Soil - Type CL from Reseda									
(1) Test No.	(2) Dead Weight lb.	(3) Base Plate Area sq.in.	(4) Soil Moisture Content w % dry wt.	(5) Resonant Frequency ω_n R.P.M.	(6) Applied Dynamic Force F_o lb.	(7) F_o W Ratio	(8) Dead Weight Contact Pressure $\frac{W}{A}$ lb./sq.in.	(9) Nominal Maximum Contact Pressure $(F_o + W)/A$ lb./sq.in.	(10) Maximum Recorded Dry Density % of max.
L11-1	670	193	14				3.47		81.2
L11-2	515	193	13	772	480	0.93	2.67	5.16	
L11-3	497	148	(a)	753 (b)	464	0.93	3.36	6.49	77.2
				772 (b)	463	0.93			
L11-3A	497	148	(a)	717	464	0.93	3.36	6.49	74.5
L11-4	436	148	(a)	680	412	0.94	2.95	5.68	71.7
L11-5	436	148	17	698	410	0.94	2.95	5.65	74.1
L11-6	436	148	17	735	490	1.13	2.95	6.26	76.3
L11-7	436	148	17	680	420	0.96	2.95	5.78	75.8
L11-8	495	148	12	890	454	0.92	3.34	6.41	73.4
L11-9	662	148	12	808	613	0.93	4.47	8.61	71.4
L11-10	686	193	12	890 (b)	630	0.92	3.55	6.82	77.8
				781 (b)	638	0.93			
L11-11	495	148	16	918 (b)	453	0.92	3.34	6.41	87.4
				781 (b)	460	0.93			
L11-12	662	148	16	863 (b)	610	0.92	4.47	8.61	86.5
				781 (b)	615	0.93			
L11-13	686	193	16	974 (b)	626	0.91	3.55	6.82	87.0
				809 (b)	640	0.93			

(continued next page)

TABLE 1.1 (CONTINUED)

SUMMARY OF DATA FROM TESTS WITH LAZAN OSCILLATORS

Soil - Type CL from Reseda

Col. 1	Col. 2	Col. 3	Col. 4	Col. 5	Col. 6	Col. 7	Col. 8	Col. 9	Col. 10
L11-14	757	148	16	671	716	0.95	5.11	9.95	86.1
L11-15	757	148	16	625	738	0.98	5.11	10.10	88.2
L11-16				No test*					
L11-17	495	148	19	616 (b)	473	0.96	3.34	6.54	80.5
				781 (b)	460	0.93			
L11-18	662	148	20	671	625	0.95	4.47	8.69	80.4
L11-19	686	193	20	671	650	0.95	3.55	6.93	78.1
L11-20	757	148	20	634	699	0.92	5.11	9.84	88.9
L11-21	757	148	20	625	703	0.93	5.11	9.87	82.9
L11-22	757	148	20	625	679	0.90	5.11	9.71	80.6
L11-23	662	148	20	776	563	0.85	4.47	8.28	80.6
L11-24	662	148	20	629	663	1.00	4.47	8.94	76.9
L11-25	662	148	20	625	683	1.03	4.47	9.09	76.8
L11-26	1105	148	20	671	804	0.73	7.47	12.90	84.8
L11-27	658	74	20	607	600	0.91	8.89	17.00	92.2
L11-28	662	148	19	625	544 (c)	0.82	4.47	8.15	92.2
L11-29	513	74	20	525	485	0.947	6.93	13.48	87.5
L11-30	513	74	20	726	341	0.665	6.93	11.54	78.3
L11-31	513	74	20	544	523	1.020	6.93	14.00	85.0
L11-32	295	74	19	707	311	1.055	3.99	8.20	82.7
L11-33	589	148	19	566	575	0.976	3.98	7.87	75.3
L11-34	769	193	20	600	649	0.844	3.98	7.34	77.7
L11-32A	295	74	20	625	521	1.090	3.99	8.34	80.2

(concluded next page)

TABLE 1.1 (CONCLUDED)

SUMMARY OF DATA FROM TESTS WITH LAZAN OSCILLATORS

Soil - Type CL from Reseda									
Col. 1	Col. 2	Col. 3	Col. 4	Col. 5	Col. 6	Col. 7	Col. 8	Col. 9	Col. 10
L11-33A	589	148	20	600	533	0.905	3.98	7.58	78.9
L11-34A	769	193	20	608	665	0.915	3.98	7.62	80.9
L11-35	662	148	18	600	646	0.976	4.47	8.84	79.5
L11-35A	662	148	18	645	588	0.888	4.47	8.44	79.9
L11-36	1180	148	18	652	763	0.646	7.97	13.14	88.2
L11-37	662	148	16	597	640	0.967	4.47	8.80	74.4
L11-38	1180	148	16	672 (d)	813	0.689	7.97	13.46	86.1
L11-38A	1180	148	16	709	904	0.766	7.97	14.09	84.6
L11-39	662	148	16	619	689	1.041	4.47	9.12	80.0
L11-40	1180	148	16	643	743	0.629	7.97	12.98	85.9
L11-41	No test*								
L11-42	662	148	15	750	569	0.860	4.47	8.31	76.5
L11-43	1180	148	15	669	797	0.675	7.97	13.35	84.0
L11-44	662	148	16	600	645	0.975	4.47	8.83	78.9
L11-44A	662	148	16	593	641	0.969	4.47	8.80	79.9
L11-45	1180	148	21	638	732	0.621	7.97	12.93	91.2
L11-46	1282	148	22	631	740	0.577	8.66	13.65	91.1
L11-47	1180	148	20 (e)	708	903	0.765	7.97	14.06	94.7

Notes: (a) Moisture content varied too widely for an average to be computed.

(b) Data from two successive runs.

(c) Oscillators forced to traverse horizontally to-and-fro across soil surface

(d) Test very unstable. Frequency shown is not resonance, but is highest frequency attained before test halted.

(e) Soil in pit initially at much higher density than in all previous tests.

* Tests were in actual fact run under these identification numbers, but were used only to test operation of, and techniques for, new assemblies of electronic measuring equipment (e.g. Brush and Miller oscillographs). No densities were measured.

TABLE 1.2

PLANNED CONDITIONS FOR TESTS WITH LAZAN OSCILLATORS

Soil - Type CL from Reseda

(1) Test No.	(2) Dead Weight	(3) Base Plate Area	(4) Desired Dynamic Force	(5) Actual Dynamic Force at Resonance	(6) Desired $\frac{F_o}{W}$ Ratio	(7) Actual $\frac{F_o}{W}$ Ratio
	W lb.	A sq. in.	F_o lb.	F_o lb.		
L11-1	670	193	670		1.00	
L11-2	515	193	515	480	1.00	0.93
L11-3	497	143	497	464(a) 463(a)	1.00	0.93 0.93
L11-3A	497	148	497	464	1.00	0.93
L11-4	436	148	436	412	1.00	0.94
L11-5	436	148	436	410	1.00	0.94
L11-6	436	148	523	490	1.20	1.13
L11-7	436	148	610	420	1.40	0.96
L11-8	495	148	495	454	1.00	0.92
L11-9	662	143	662	613	1.00	0.93
L11-10	686	193	686	630(a) 638(a)	1.00	0.92 0.93
L11-11	495	148	495	453(a) 460(a)	1.00	0.92 0.93
L11-12	662	148	662	610(a) 615(a)	1.00	0.92 0.93
L11-13	686	193	686	626(a) 640(a)	1.00	0.91 0.93
L11-14	757	148	757	716	1.00	0.95
L11-15	757	148	908	738	1.20	0.98
L11-16			No test*			
L11-17	495	148	495	473(a) 460(a)	1.00	0.96 0.93

(continued next page)

TABLE 1.2 (CONTINUED)

PLANNED CONDITIONS FOR TESTS WITH LAZAN OSCILLATORS

Soil - Type CL from Reseda

Col.(1)	Col.(2)	Col.(3)	Col.(4)	Col.(5)	Col.(6)	Col.(7)
L11-18	662	148	662	625	1.00	0.95
L11-19	686	193	686	650	1.00	0.95
L11-20	757	148	757	699	1.00	0.92
L11-21	757	148	908	703	1.20	0.93
L11-22	757	148	757	679	1.00	0.90
L11-23	662	148	530	563	0.80	0.85
L11-24	662	148	795	663	1.20	1.00
L11-25	662	148	1324	683	2.00	1.03
L11-26	1105	148	1105	804	1.00	0.73
L11-27	658	74	658	600	1.00	0.91
L11-28(b)	662	143	662	544	1.00	0.82
L11-29	513	74	513	485	1.00	0.947
L11-30	513	74	308	341	1.00	0.665
L11-31	513	74	769	523	1.00	1.020
L11-32	295	74	295	311	1.00	1.055
L11-33	589	148	589	575	1.00	0.976
L11-34	769	193	769	649	1.00	0.844
L11-32A	295	74	295	321	1.00	1.090
L11-33A	589	148	589	533	1.00	0.905
L11-34A	769	193	769	665	1.00	0.915
L11-35	662	148	662	646	1.00	0.976
L11-35A	662	148	662	588	1.00	0.888
L11-36	1180	148	1180	763	1.00	0.646
L11-37	662	148	662	640	1.00	0.967
L11-38	1180	148	1180	813	1.00	0.689
L11-38A	1180	148	1180	904	1.00	0.766
L11-39	662	148	662	689	1.00	1.041
L11-40	1180	148	1180	743	1.00	0.629

(concluded next page)

TABLE 1.2 (CONCLUDED)

PLANNED CONDITIONS FOR TESTS WITH LAZAN OSCILLATORS

Soil - Type CL from Reseda

Col.(1)	Col.(2)	Col.(3)	Col.(4)	Col.(5)	Col.(6)	Col.(7)
L11-41			No test*			
L11-42	662	148	662	569	1.00	0.860
L11-43	1180	148	1180	797	1.00	0.675
L11-44	662	148	662	645	1.00	0.975
L11-44A	662	148	662	641	1.00	0.969
L11-45	1180	148	1180	732	1.00	0.621
L11-46	1282	148	1282	740	1.00	0.577
L11-47	1180	148	1180	903	1.00	0.765

- Notes: (a) Data from two successive runs.
 (b) Oscillator forced to traverse horizontally to-and-fro across soil surface.
 * See note under Table 1.1

drive. Circular base-plates and rectangular dead-weight plates were provided to give variation of the base-plate area and total dead weight of the oscillating unit. Frequency of vibration was observed by means of a tachometer electrically driven by the output of a small generator geared directly to one of the rotating shafts of the Lazan oscillator, and the displacements were measured by means of a Consolidated Engineering Company Velocity Pick-up and Vibration Meter. A tall guide-rod was screwed in a vertical position to the top plate of the whole oscillator assembly. Gentle application of force near the top of the guide-rod in the direction in which the oscillator was tending to move caused a reversal of motion, and hence provided control of unwanted lateral movements. This method had proved singularly successful in the work with the sandy loam, but was less successful in the tests on the Reseda CL soil due to the tendency for the oscillator to tilt and "dig-in" to the soil when the force, however gentle, was applied to the rod. An illustration of the complete assembly is shown on Plate 1.1. This is a photograph of an earlier test on sandy loam, the large tripod and the level for settlement measurements being dispensed with in the work on the Reseda CL soil.

Dynamic force was provided by the rotation of two shafts in opposite directions, eccentric weights being mounted on both shafts in such a manner that the force vector was maintained in a plane perpendicular to the oscillator base, there being no horizontal component of this vector. Brass eccentric weights were at first utilized, but were later replaced by heavier ones made of lead. The effective dynamic force at any given speed of rotation could be varied by means of a dial on the exterior of the vibrator. Readings on the dial in degrees (Θ) supplied the necessary data for calculating the dynamic force by means of the equation:

$$F_o = 3.428 \omega^2 \sin \frac{\Theta}{2} \text{ pounds} \quad (1.1)$$

where ω = frequency in cycles per second

In the first seven tests it was found that completely inadequate compaction was obtained with the above equipment. There was a definite limit to the dynamic force available at a given frequency, and this provided a very severe limitation on the investigations. It soon became clear that appreciable compaction was not being obtained with the dead weights and contact pressures being used in the first few tests. The base area could of course have been reduced, but this was felt to be, and later established as, an

undesirable procedure. The other alternative was to increase the dead weight and dynamic force. However, by doing so, it was clear that the resonant frequency would be reduced. In fact it was reduced to a value lower than the minimum frequency required to develop the desired dynamic force. Table 1.2 shows that the desired dynamic force in Test L11-7 was 610 pounds requiring, with maximum available moment of eccentricity, a frequency of 820 R.P.M. At any higher frequency than this, the dynamic force could be maintained constant by reducing the angle θ in accordance with equation (1.1). However, in that particular test, resonance occurred at a frequency of 680 R.P.M. resulting in a dynamic force of only 420 pounds.

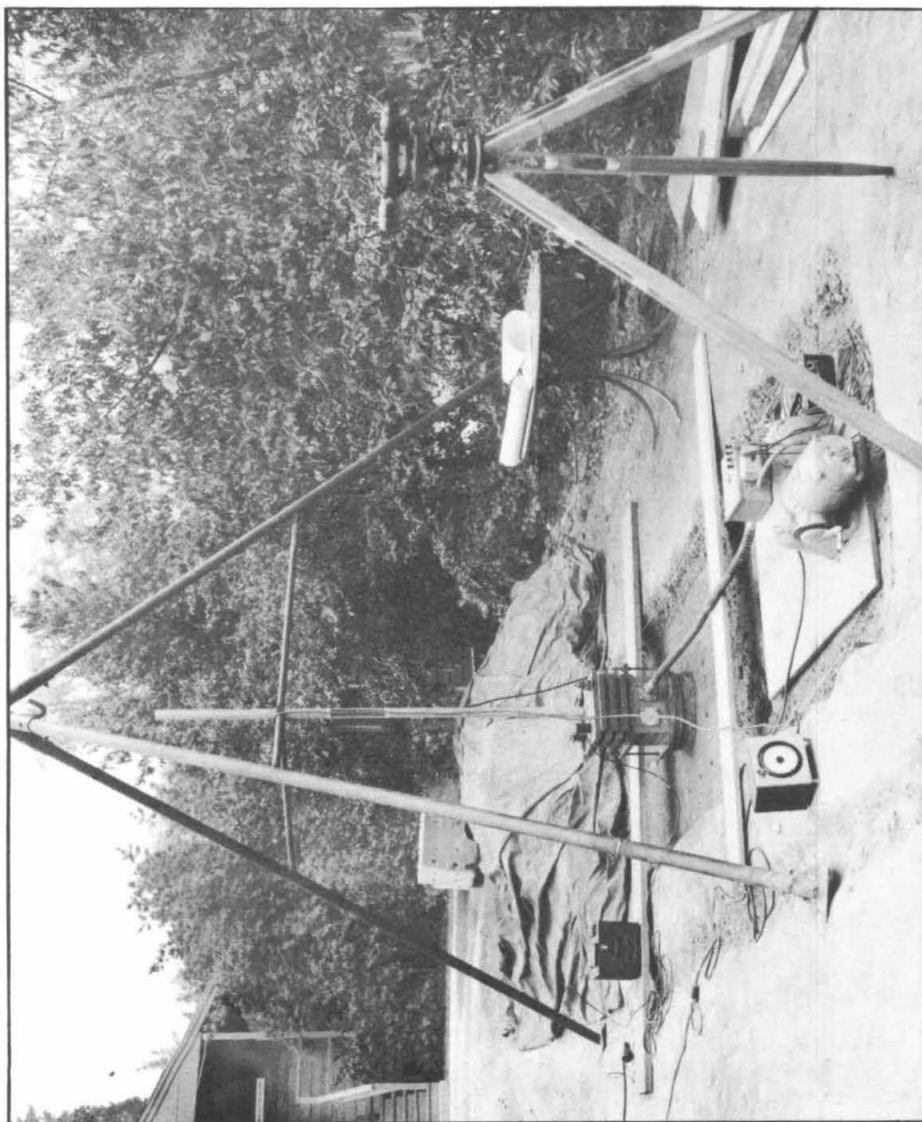
Consideration was then given to methods of obtaining a higher available moment of eccentricity, so that at any given frequency a larger dynamic force would be available than with the equipment on hand. Sufficient resources not being available for the development of a new machine, a second Lazan oscillator was obtained from the U. S. Navy and geared to the first oscillator, one oscillator being placed directly on top of the other. The same 1 H.P. motor and transmission was used for the two oscillators as for the one, mainly due to the cost and difficulties of obtaining items designed for heavier and more powerful duties. The motor was found adequate for the purpose providing that the angular eccentric setting at the start was made less than 70° , so that the dynamic unbalance was smaller than that of one oscillator at its maximum angular setting (approximately 140°). The motor was designed to operate one Lazan when at its maximum angular setting.

As may be seen on Plate 1.2, much of the dead weight was provided by steel plates supported on the top of the Lazan oscillators. It will also be observed that other electronic equipment was mounted on the oscillators, in addition to the one velocity pick-up mentioned earlier. A full discussion of this additional equipment is given in section 1.9.3 of this chapter.

1.6.2 Procedure

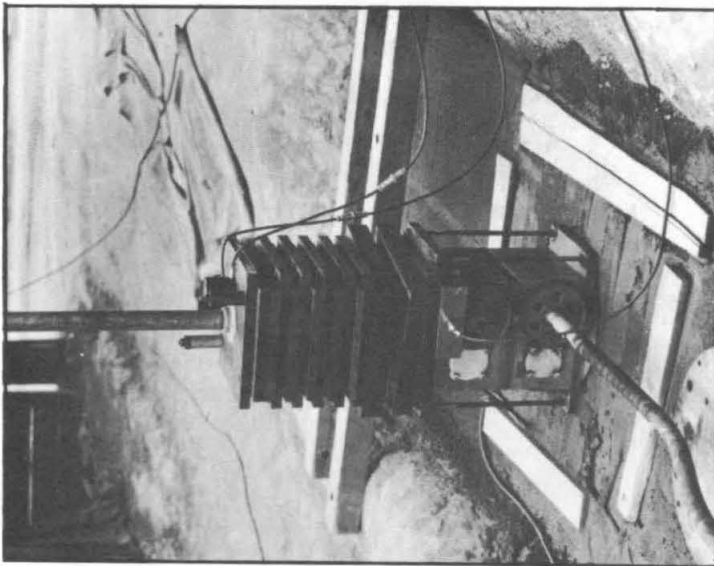
The pit was filled carefully at a moisture content about 0.5% higher than desired, to allow for evaporation losses, and the last lift was very carefully levelled and rolled.

The base-plates were positioned in the center of the pit laterally, but not longi-

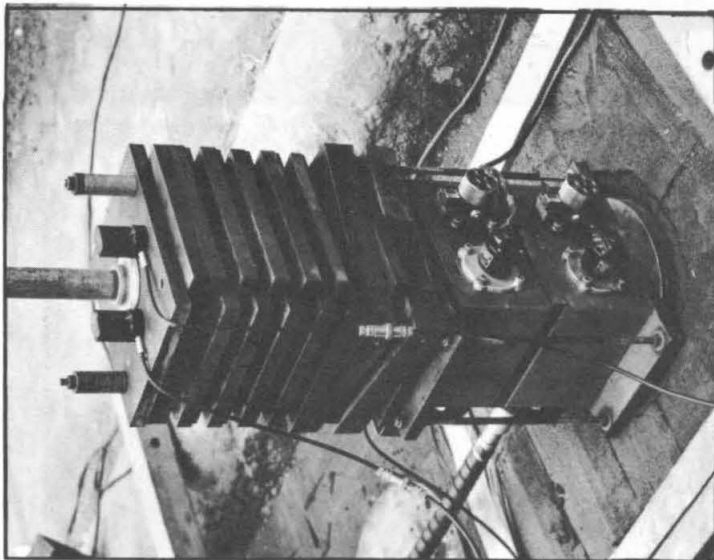


Equipment Assembly using One Iazan Oscillator,
with Electrical Instruments to Measure Frequency and Displacement.

PLATE 1.1



(A) Equipment Assembly using Two Lazan Oscillators geared together. The Impulse Pick-Up is mounted on the Bracket covering the Top of the Upper Gear Wheel.



(B) Equipment Assembly using Two Lazan Oscillators geared together. The Dials showing Angular Eccentricity and the Knurled Control Knobs can be seen. Two Velocity Pick-Ups are mounted on the Top Dead Weight Plate.

tudinally for reasons given later, there being formed a stack of plates of the same diameter at least 5 inches high to allow settlements to that depth to occur unhindered by other plates of different shape or size. Settlement to such a depth may be seen in Plate 1.2.

After completing the assembly with all necessary dead weight, the shafts were set in motion at a low frequency (about 300 R.P.M.), and the angular eccentricity was set at the highest possible figure. The frequency was then increased in increments of 30 R.P.M., taking displacement readings after each increment, until either resonance was reached or the frequency was reached at which the desired dynamic force was being developed. After this latter frequency was reached, the angular eccentricity setting was adjusted, so that when the next increment of frequency was added, the desired constant force F_o was obtained in accordance with the equation:

$$F_o = 6.856 \omega^2 \sin \theta / 2 \quad (1.2)$$

1.6.3 Density Measurements

Immediately following the completion of the cycle of vibrations, densities were taken in the soil to a depth of 18 inches below the original ground surface. Great reliance was placed on the core-cutting method using stainless steel seamless cylinders, 2 inches O.D. by 2 inches long with #18 gauge wall thickness. Preliminary tests had shown that uniformity and accuracy was possible using this method in the Reseda CL soil. Check tests were also made with the sand-replacement method.

It had been hoped that the penetrometer method could be used to determine values of density. However, calibration tests showed that the slope of the penetration-density curve was very steep when the soil density exceeded about 90% of maximum, so that a very small change in rate of penetration represented a relatively large change in density. Since a certain amount of scatter of data is inevitably present when using a penetrometer, its use was not continued.

Penetrations in the soil adjacent to the points where densities were being measured were made with a Proctor Needle. This was done mainly to obtain a quick idea as to the effectiveness of the compactive effort under the particular test conditions, but was also used to show the "spread" of the compactive effort and to show up any undue variations of this "spread" that might require special thought and investigation.

1.6.4 "Spread" of Compactive Effect

Under the original planning, two tests with the Lazan oscillator were to be conducted on each pit full of prepared soil. However it was eventually possible to make three tests as the circumstances warranted. Under these conditions, the distance between the positions of the individual Lazan test sites was 32 inches, or twice the diameter (15.75 inches) of the largest base-plate utilized. Originally the feasibility of conducting three tests at each filling of the pit was questioned because of the possibility of some measure of lateral spread of the compactive effect in one test interfering with an adjacent test. Such a spread was shown not to exist with the Reseda CL soil, density and Proctor Needle measurements indicating that the only measurable changes in soil density occurred directly underneath the base plate of the oscillator.

1.7 Contact Pressures and the Necessity to Operate at Resonance

The compaction of cohesive soils is a problem of supplying sufficient stress within the soil mass to overcome the shearing strength of the material and cause the soil particles to readjust into a more compact mass. In this respect the problem differs from that of the compaction of sand, since vibrating sand particles will readjust to a compact condition under the forces of gravity alone. Vibration compaction of cohesive soils has an advantage over singly applied stresses, as in an orthodox roller, because of repetitive action. The force is applied and released and applied again, many times. It is a well known fact from laboratory compression tests or field load tests that each release and reapplication of load results in greater settlement.

Both the theory of vibrations and field test experience indicate that operation at resonant frequency is essential if adequate compaction of soil is to be achieved by the vibration process, with the least expenditure of energy and the lightest equipment. In every phase of the work at the California Institute of Technology the greatest settlements and the highest densities have been obtained when the vibrator-compactor has been operating at resonant frequency.

The reason for this is clear from a consideration of the general theory of vibration, as discussed in previous reports.^{(1,2)*} There is a much larger magnification

* The numbers in parenthesis refers to the list of references at the end of this chapter.

of the impressed dynamic force at resonance than at other frequencies, hence the stresses within the soil should be greater and compaction more effective. While there is little in the published literature to indicate that a comprehensive study has ever been made of the pressures within the soil due to surface vibration over a wide range of frequencies, there are a few cases where pressure measurements have been taken.

Pauw⁽³⁾ measured surface pressures beneath a concrete block resting on sand and subjected to a sinusoidal vertical impressed vibration giving a resonant condition for vibrator, block, and soil. His results show magnifications of dynamic stress of from 1.58 to 4.66 even though the applied force was low compared to the dead weight of vibrator and block. Table 1.3 shows the results of these tests.

TABLE 1.3

DATA FROM EXPERIMENTS BY PAUW

Dead Weight W	Base-Plate Area A	Dynamic Force F	Apparent Dynamic Contact Pressure $f_1 = F/A$	Measured Dynamic Contact Pressure f_2	Magnification Factor f_2/f_1
lb.	sq. ft.	lb.	lb./sq. ft.	lb./sq. ft.	Ratio
700	2.25	300	133	620	4.66
860	2.25	300	133	240	1.80
1025	2.25	300	133	210	1.58
1150	3.75	300	80	180	2.25
1900	6.25	500	80	235	2.94
2600	8.75	500	57	208	3.65
3600	12.25	600	49	125	2.55

Whiffin⁽⁴⁾ measured pressures at a depth of 8 inches beneath a roller weighing 2180 pounds and equipped with a rotating eccentric shaft operating at 4800 to 5500 cycles per minute. Even though the vibrations were far above resonance, the amplification was approximately 2.0.

Bernhard and Finelli⁽⁵⁾ measured pressures at a depth of 18 inches below

a vibrating plate and found that there was a close resemblance between the curve of pressure at various frequencies and the vibrator displacement at those frequencies.

From the above discussion the desirability of operating at resonance of the vibrator soil mass is clear, and the remaining problem is to determine the required contact pressures between soil and vibrator.

1.7.1 Theoretical Considerations

The reasoning behind the concept of what takes place during vibration compaction of cohesive soils is based on well-known theoretical and experimental considerations of stress distribution beneath a loaded plate; the occurrence of plastic action within the soil when the shearing strength has been exceeded; the magnification of soil pressures at resonance; and the impulsive stresses of compression and tension set up by impact.

The shear stress pattern beneath a loaded plate is shown on the left half of Figure 1.3 for a circular plate under a static load on a homogeneous isotropic medium with one surface. The actual stress distribution, of course, is not exactly the same because the theoretical conditions are not met in the ordinary soil. However, the general pattern is correct, and will be used in this discussion.

The shearing strength of the soil that is being compacted may be considered mainly dependent upon its cohesion. It is doubtful if the full value of the frictional strength of the soil is developed, or if it exists at all, because of two factors, namely:

- (i) The condition of alternating compression and tension during oscillation;
- (ii) the normal pressure on the slip plane at the beginning of plastic deformation is low. Plastic deformation commences at the edge of the base-plates and rapidly extends deeper into the soil as settlements increase. As can be seen from Fig. 1.3, the vertical and horizontal external forces at the edge of the plate are zero, hence no frictional strength can be developed in the soil. Certainly it is doubtful if the exact value of internal friction could be evaluated because of these conditions, and the consequent uncertainty as to the condition of stress when the impulsive force is applied. Assuming that the entire strength of the soil is due to its cohesion, it is apparent that the greater the cohesion the more force is required to develop plasticity. Again referring to Fig. 1.3 the maximum shearing stress extends along an elliptical arc from

the edges of the plate to a depth of about $3/8$ the width of the plate below the surface. Its value is equal to the surface load divided by π . The stress at any other point within the soil will be at a lower value. For instance, at 100 pounds per square inch vertical soil pressure, the shearing stress at a depth of 1.2 times the width of the plate is $1/10$ th of the vertical pressure, or 10 pounds per square inch. Plastic action will start at the edges of the plate and progress downward into the soil, following the general curve of maximum shearing stress but deviating from it because the pressure distribution at the surface will change as plasticity progresses. The cohesive strength of the soil increases with increasing density of the soil at a given moisture content. Some compaction will therefore occur at low unit compressive stresses, but as the density increases, higher compressive stresses are required. The depth to which compaction can extend is also limited by the surface pressure. For instance, when the soil from the pit was compacted to a maximum density of 112.8 pounds per cubic foot at 18% moisture the cohesive shearing resistance was 9.7 pounds per square inch. Compaction should then be expected to start along the line of the maximum shear stress under a normal surface load of 30 pounds per square inch. However, if the compaction is to extend to a depth of 1.2 times the width of the plate, a unit surface pressure of 96 pounds per square inch is required. If only 46 pounds per square inch of normal surface pressure were applied, compaction would not be expected to a depth greater than $3/4$ the width of the plate.

From the above it is clear that forces of fairly large magnitude must be transmitted into the soil if compaction to any considerable depth is to be expected. To obtain the required forces with the vibrator used in these tests large magnifications of the dynamic force are necessary. These are only available when operating at the resonant frequency of the vibrator-soil mass. If the maximum dynamic force is 10 pounds per square inch on the vibrator base, a magnification of at least three times is necessary to start compaction of this soil; of $4-1/2$ times to cause the compaction to extend to $3/4$ of the width of the plate; and of nearly ten times to cause compaction to extend to $1-1/4$ times the width of the plate.

A maximum density of 112.8 pounds per cubic foot at an optimum moisture

of 14.6% was obtained for the soil of these tests by the modified A.A.S.H.O. method. The maximum possible moisture at this density, with zero air voids, is about 18%. Since cohesion decreases with increase in moisture content of the soil, it has been found desirable to work on the wet side of optimum, and as close to the limit of saturation as possible, thereby getting the greatest amount of compaction with the lowest possible vibrator forces.

1.8 Measurement of Contact Pressures

The simplest and most straight-forward method of obtaining the contact pressure between the vibrator and the soil appeared to be to place a pressure cell in the base of the vibrator and to record the pressures electronically. An attempt to use an available pressure cell was unsuccessful, due to trouble with the cell, and since neither time nor funds were available to go into this matter extensively, no measurements are available from these tests.

1.9 Calculation of Contact Pressures

Following the failure to directly measure contact pressures, recourse was made to the mathematical theory, and it was observed that if the following equations could be solved, values of contact pressure could be computed:

$$k = \frac{F_o}{\delta \sqrt{\left\{1 - \left(\frac{\omega}{\omega_n}\right)^2\right\}^2 + \left\{2c\left(\frac{\omega}{\omega_n}\right)\right\}^2}} \quad (1.3)$$

$$\bar{F} = k \times \delta \quad (1.4)$$

With all terms on the right-hand side of equation (1.3) being easily measured, except for the damping ratio, c , the problem lay in the determination of this quantity. Two methods were brought into use, known respectively as the "Displacement Analysis Method" and the "Phase-Angle Analysis Method."

1.9.1 Linear and Non-Linear Vibrating Systems

Before entering a detailed description of these methods, it must be pointed out that one assumption is implicate in all this work. That is that the vibrator-soil

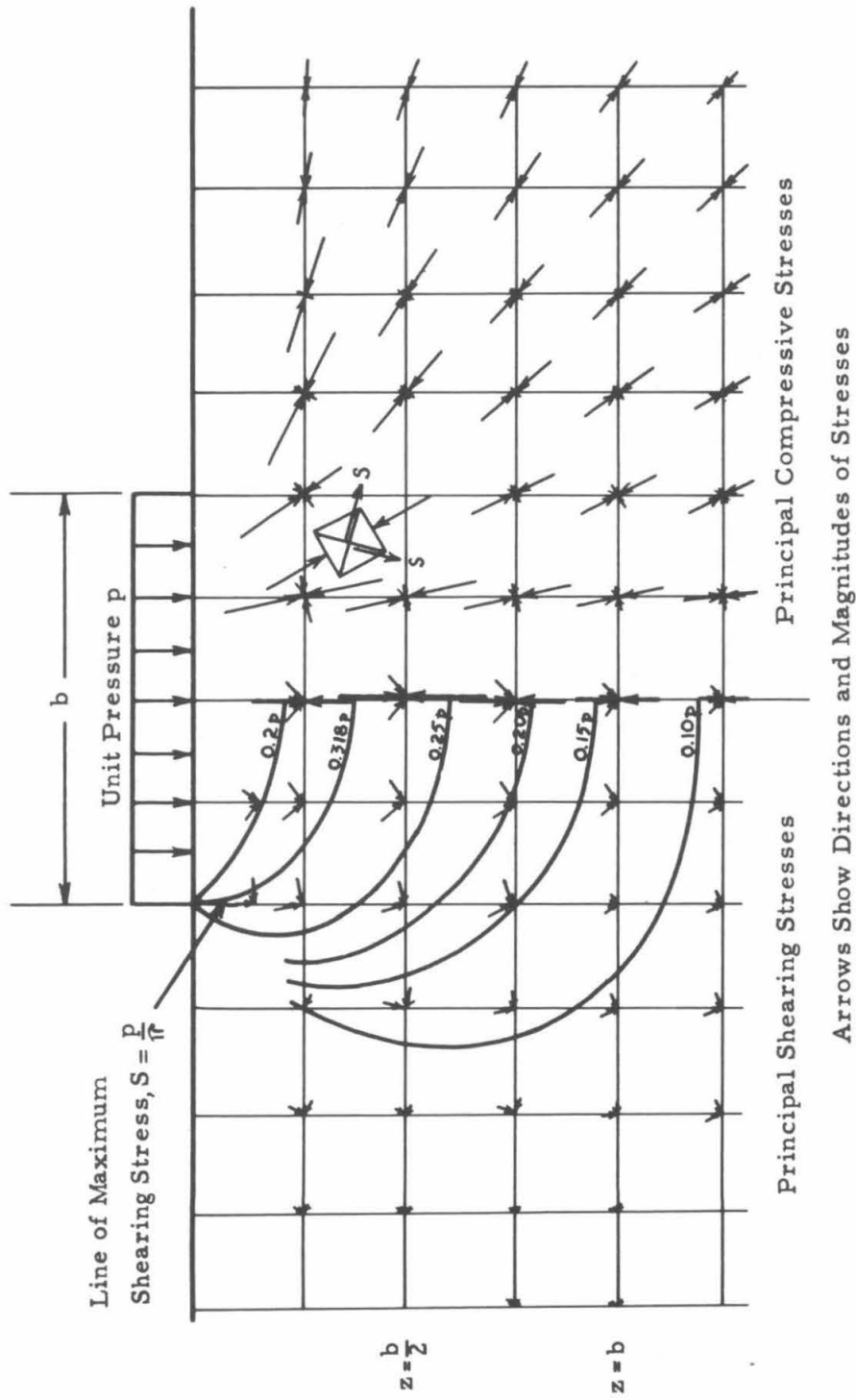


Fig. 1.3 DISTRIBUTION OF STRESSES UNDER A LOADED CIRCULAR AREA

system vibrates in a linear manner, by which is meant that the damping of the system is directly proportional to the velocity of the motion. A number of factors, particularly the shape of the displacement-frequency curves, indicate that this was not strictly the case in the tests described in this chapter. Fig. 1.4 shows a set of theoretical curves for an ideal linear vibrating system with various damping factor ratios, upon which has been superimposed the curve from one of the Lazan tests. The distortion of the test curve is a measure of the amount of non-linearity existing in the vibrator-cohesive soil system. In spite of this, it was felt that rejection of the existing theories was not justified, as the development of a new theory for a non-linear vibrator-soil system would be a lengthy process and would not necessarily give any greater accuracy ultimately due to the various degrees of non-linearity exhibited from test to test. Moreover, a number of other factors indicated that the departure from a linear system was not excessive. Thus Plate 1.3, which is a photograph of a trace showing a typical time-displacement relationship for the resonant condition in a Lazan test, shows that the vibrating motion was not significantly different from a sinusoidal motion. Since the time-force relationship of the applied dynamic force was of a sinusoidal nature, it was anticipated that the resulting motion would be of the same type if the system were linear, or approximately linear.

Accordingly the linear theory was accepted in this work, so that the vibrator soil system was considered in terms of an equivalent linear system, and all factors were calculated on that basis. Although any solutions arrived at in this way must necessarily contain a margin of error, this was not felt to be any greater than would be the case if a non-linear theory of vibrations were to be developed. For if such a step were taken, an assumption would have to be made as to the manner in which the system was non-linear, e.g. by assuming the damping to be proportional to the square of the velocity of motion, and if this assumption were incorrect, then any solution arrived at would give an equivalent non-linear system of the type of non-linearity assumed at the outset. Clearly, no greater accuracy would be assured in this manner than would be obtained by the method actually used.

1.9.2 Displacement Analysis Method for Calculating Contact Pressures

In the previous work with a vibrator operating on sand, the value of the damping factor ratio had been determined for the resonant condition by comparing the peakedness of the test displacement-frequency curves with those of the theoretical curves for linear systems with various known damping factor ratios. Such a comparison is shown in Fig. 1.4 for Test L11-47. However this comparison only provided information about the resonant condition of the system, and hence did not show the relation between the values of the spring constant, effective dynamic force, and other parameters at resonance and at other frequencies.

By a simple extension of the procedure, it was seen readily possible to determine the damping factor ratios at frequencies other than resonance. Thus, in Fig. 1.4, the test curve plotted for the data of Test L11-47 intersects, at a frequency ratio (ω/ω_n) of 0.8, the theoretical curve for a system with a damping factor ratio of 0.03. It is assumed for this analysis that if the vibrator-soil system represented by the conditions existing in Test L11-47 be operated at the frequency represented by the frequency ratio of 0.8, then that vibrator-soil system is equivalent to a linear vibrating system with damping factor ratio 0.03. Since for the particular frequency ratio under consideration the values of applied dynamic force and amplitude of vibration are known, equations (1.3) and (1.4) can be solved, and the existing effective dynamic force, which is some multiple of the applied dynamic force, is established. The existing effective dynamic contact pressure is then calculable. A similar argument is forwarded for other frequencies above and below resonance, enabling the comparative effect of operating at resonance to be determined.

A typical calculation for the range of contact pressures above and below resonance is shown in Tables 1.4 and 1.5, which present the data for Test L11-47. The procedure in carrying out the analysis is as follows:

(a) The basic measurements of frequency and displacement are entered in Table 1.4. Values of dynamic force are known for the given frequencies.

(b) Values of "normalised" amplitude are computed and entered in column (5) of Table 1.4. This "normalisation" is necessary since the linear theory of vibrations is based on the presence of a dynamic force of constant value, whereas due to

TABLE 1.4

BASIC DATA FROM TEST L11-47

(1) Frequency	(2) Frequency	(3) Applied Dynamic Force F_o	(4) Displacement peak-to-peak 2δ	(5) Normalised Amplitude δ/F_o	(6) Frequency Ratio ω/ω_n	(7) Amplitude Ratio $(\frac{\delta}{F_o})/(\frac{\delta}{F_o})_n$
c.p.s	R.P.M.	lb.	mils.	in./kip		
7.70	462	383	14	0.0183	0.639	0.1075
8.50	510	467	20	0.0214	0.705	0.1257
9.83	590	625	35.5	0.0284	0.816	0.1668
11.26	676	821	77	0.0469	0.935	0.2754
12.05	723	940	320	0.1703	1.000	1.0000
13.01	781	1096	300	0.1369	1.080	0.804
14.09	847	1198	250	0.1044	1.171	0.613
15.08	905	1193	225	0.0943	1.251	0.554
16.08	965	1194	196	0.0821	1.335	0.482
17.06	1025	1189	171	0.0719	1.418	0.422
18.04	1083	1187	151	0.0636	1.498	0.373

the limitations of the equipment used, the dynamic force was generally increasing as the frequency increased. "Normalisation" consists of dividing the measured amplitude by the corresponding applied dynamic force, thereby presenting the motion in terms of a constant unit dynamic force. The unit of force in this case is the Kip (1000 pounds).

(c) The curve of normalised amplitude vs. frequency is plotted, Fig. 1.5 to verify whether or not the resonant frequency is that at which the maximum normalised amplitude was measured. Such is generally the case, but as Fig. 1.6 shows for Test L11-45, a smooth curve drawn through the plotted test data indicates resonance to be slightly lower (10.75 c.p.s.) than the frequency corresponding to the highest measured normalised amplitude (11.1 c.p.s.)

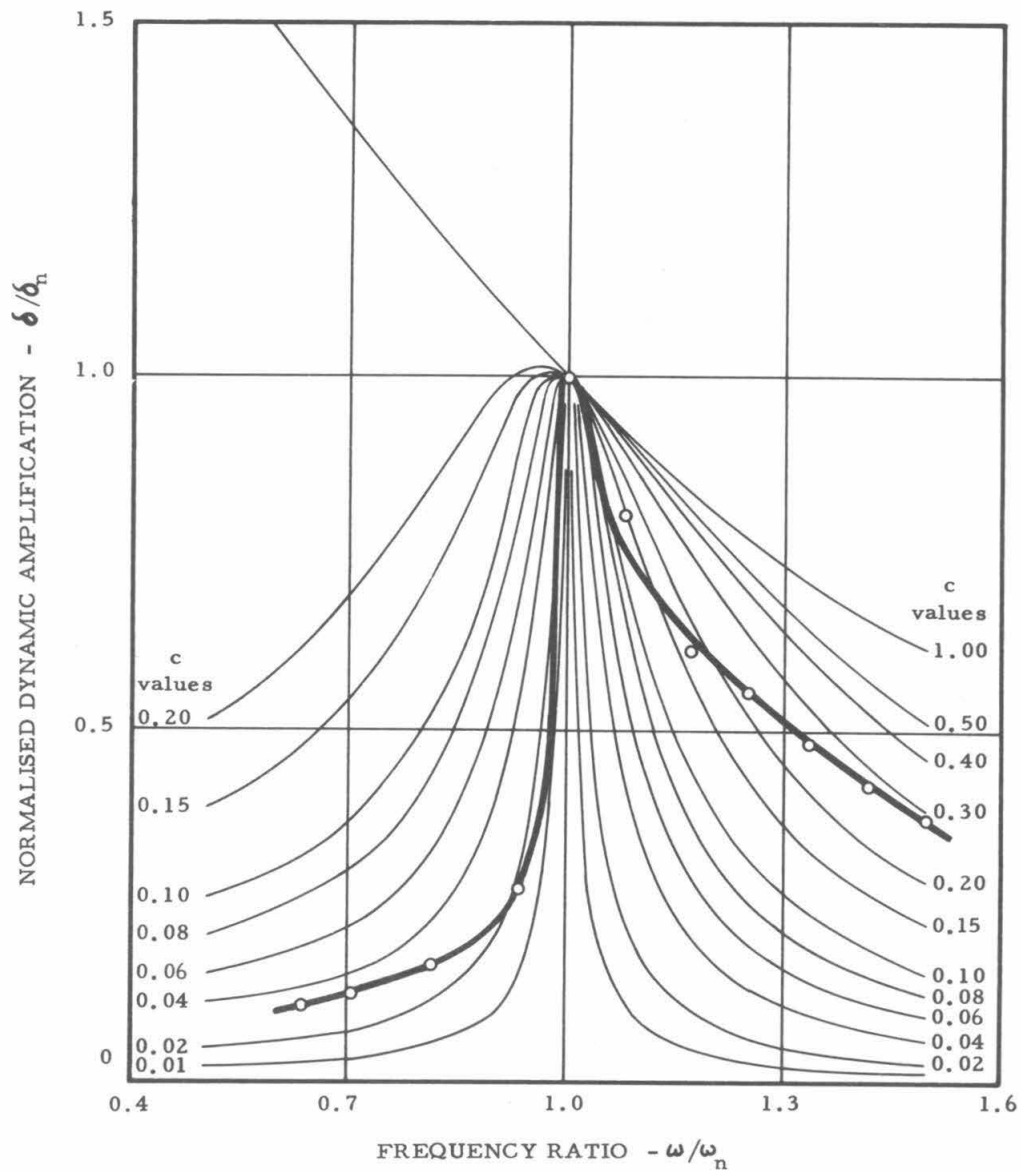


Fig. 1.4 RELATIONSHIP BETWEEN FREQUENCY RATIO AND AMPLITUDE RATIO,
COMPARISON BETWEEN THEORETICAL CURVES FOR A LINEAR
SYSTEM WITH VARIOUS DAMPING FACTOR RATIOS AND
THE TEST CURVE FROM TEST L11-47

(d) After establishing the resonant frequency and the corresponding normalised amplitude, columns (6) and (7) in Table 1.4 are computed.

(e) From columns (6) and (7) of Table 1.4, the curve of amplitude ratio vs. frequency ratio is drawn, and compared with the theoretical curves of this type, as in Fig. 1.4. Values of the damping factor ratio corresponding to a frequency ratio where the test curve intersects a theoretical curve of known damping factor ratio are then abstracted and entered in column (2) of Table 1.5, with the corresponding frequency ratios in column (1).

(f) The curve showing the relationship between applied dynamic force and frequency ratio is plotted, Fig. 1.7, from the data in Table 1.4, and the force values corresponding to the frequency ratios in Table 1.5 are entered in column (3).

(g) The normalised amplitudes corresponding to the frequency ratios in Table 1.5 are taken from the curve plotted to show this relationship, Fig. 1.8, and are entered in column (4). Since, however, the units of amplitude are required in inches, and not in inches per kip, the values in column (4) are multiplied by the corresponding values of dynamic force, and the results entered in column (5).

(h) The calculations then follow as indicated by the headings of the succeeding columns in Table 1.5, the last three columns showing, respectively, the effective dynamic force, the number of times bigger this force is than the applied dynamic force, and the contact pressure generated by this force between the base of the vibrator and the soil surface.

1.9.3 Phase-Angle Analysis Method for Calculating Contact Pressures

The frequency ratio, damping factor ratio, and phase angle of a linear vibrating system undergoing sinusoidal motion are related by the equation:

$$\tan \phi = \frac{2c \left(\frac{\omega}{\omega_n} \right)}{1 - \left(\frac{\omega}{\omega_n} \right)^2} \quad (1.5)$$

The phase angle is the angle between the vector representing the applied dynamic force and the vector representing the resulting vibrations, and the basic definition of resonance is "that frequency at which the phase angle is exactly 90° ." There are three values

TABLE 1.5
CALCULATION OF DYNAMIC AMPLIFICATION FACTORS - TEST L11-47

(1) Fre- quency Ratio	(2) Damping Factor Ratio	(3) Applied Dynamic Force	Displacement Analysis Method					(9) Spring Constant (3)	(10) Effective Dynamic Force (=kδ)	(11) Dynamic Amplifi- Factor	(12) Dynamic Effec- tive Unit Dynamic Contact Pressure
			(4) Normal- ized Amplitude $\frac{\delta}{F_o}$	(5) Ampli- tude $\frac{\delta}{F_o} \times F_o$	(6) $(1 - [\frac{\omega}{\omega_n}]^2)$	(7) $(2c \frac{\omega}{\omega_n})^2$	(8) $\sqrt{(6)+(7)}$				
ω/ω_n	c	F_o lb.	in./Kip	δ in.				k lb./in.	\bar{F} lb.	\bar{F}/F_o	p.s.i.
0.80	0.03	580	0.0275	0.0160	0.4095	0.0015	0.7148	50,875	814	1.40	5.50
0.90	0.025	760	0.0400	0.0304	0.0361	0.0016	0.1942	128,815	3,916	5.15	26.46
1.00	0.02	940	0.1703	0.1601	0	0.0016	0.0400	146,875	23,515	25.02	158.89
1.04	0.08	1015	0.1550	0.1573	0.0066	0.0277	0.1851	34,880	5,487	5.41	37.07
1.06	0.10	1050	0.1460	0.1533	0.0151	0.0538	0.2624	26,120	4,004	3.81	27.05
1.12	0.15	1160	0.1220	0.1415	0.0641	0.1413	0.4530	18,095	2,560	2.21	17.30
1.20	0.20	1190	0.1020	0.1214	0.1936	0.3320	0.7250	13,525	1,642	1.38	11.09

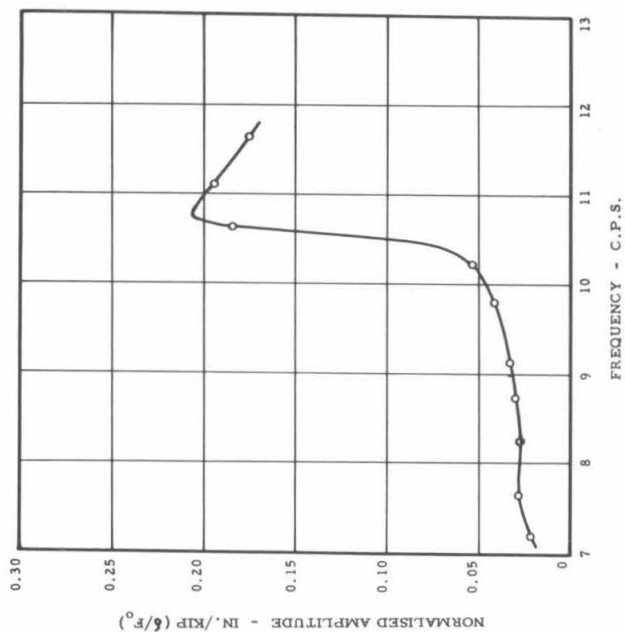


Fig. 1.6 RELATIONSHIP BETWEEN FREQUENCY AND NORMALISED AMPLITUDE,
TEST L11-45

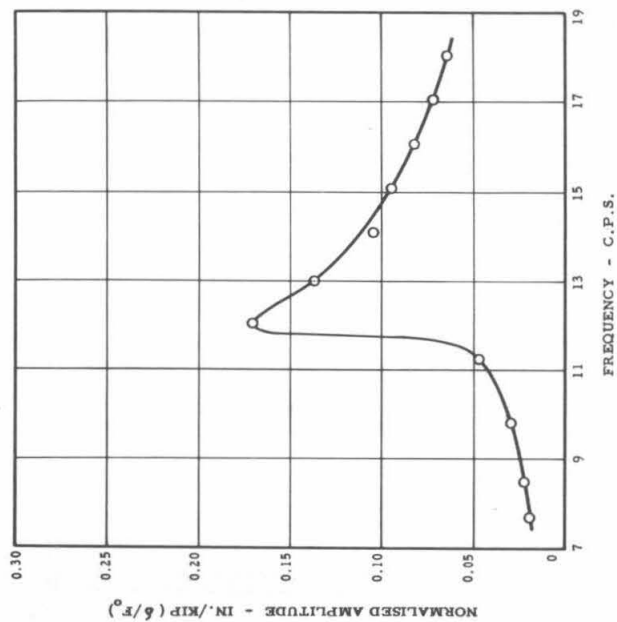


Fig. 1.5 RELATIONSHIP BETWEEN FREQUENCY AND NORMALISED AMPLITUDE,
TEST L11-47

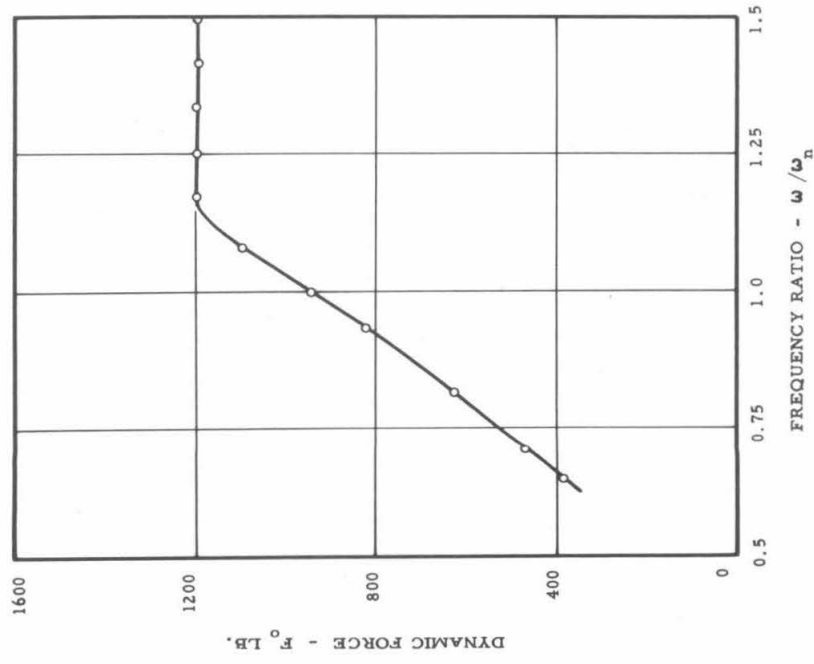


Fig. 1.7 INCREASE IN DYNAMIC FORCE WITH INCREASE IN FREQUENCY, TEST L11-47

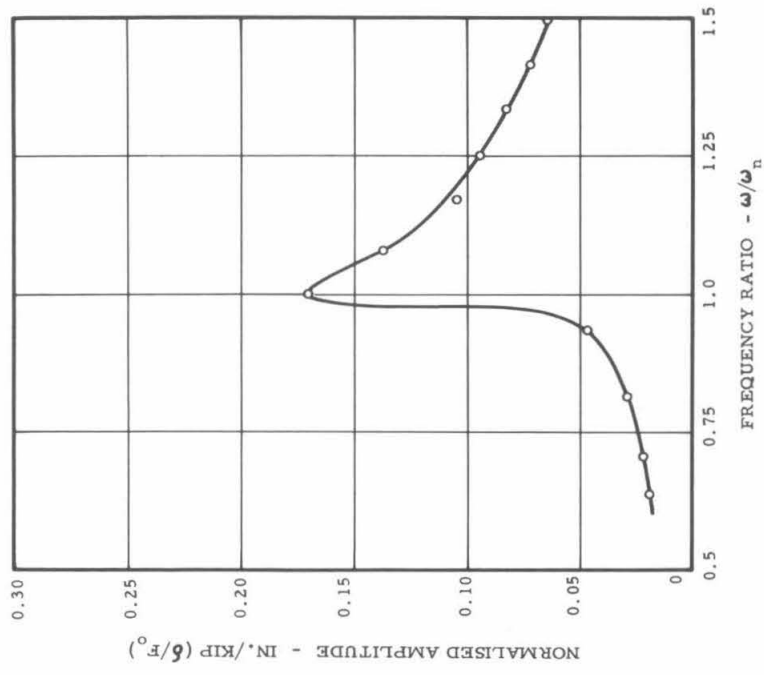


Fig. 1.8 RELATIONSHIP BETWEEN FREQUENCY RATIO AND NORMALISED AMPLITUDE, TEST L11-47

of the frequency ratio for which the phase angles are equal for all damping factor ratios. For $(\omega/\omega_n) = 0$, $\phi = 0$; for $(\omega/\omega_n) = 1$, $\phi = 90^\circ$; and for $(\omega/\omega_n) = \text{infinity}$, $\phi = 180^\circ$. For all other values of the frequency ratio, the relationship with the phase angle is uniquely a function of the damping factor ratio, and there exists a family of curves relating frequency ratio to phase-angle, analogous to the family of curves relating frequency ratio to amplitude ratio (for various damping factor ratios). Some of this family of curves are shown in Fig. 1.9.

The use of the phase-angle relationships was very advantageous in this later stages of the test program. In the first place, measurement of the phase-angles during the tests enabled the resonant frequency to be very accurately established. Secondly, the shape of the phase angle curves is much simpler than that of the amplitude ratio curves, and the portion of the curves in the vicinity of resonance is very nearly a straight line. On this account more accurate tests curves could be constructed and a more accurate comparison made at the resonant frequency.

The method of calculating dynamic amplification and contact pressures being identical to that outlined in section 1.9.2 of this report, the only problem lay in measuring the phase angles during the tests. Various means were attempted, the first of which involved the simultaneous recording on an oscillograph chart of the time-displacement, time-velocity, and time-acceleration relationships existing during the vibration tests. Considerable difficulties were experienced with the instruments used to record these relationships, and no success was achieved. Eventually a method was devised using a magnetic pick-up impulse generator, and this proved successful.

The magnetic pick-up impulse generator consists of a permanent magnet energizing a pole piece surrounded by a coil of wire. When the external magnetic field of this device is distorted by the movement of a metallic object past the end of the pole piece, a voltage output is generated proportional to the speed of the object. The object must be made of a metal capable of being magnetized.

In the determination of phase-angles, a small steel screw was screwed into the side of the external gear wheel on the upper Lazan, as close to the periphery as possible. The impulse pick-up was mounted on a bracket attached to the upper cover plate of the Lazan assembly, in such a manner that the center of the pole piece was

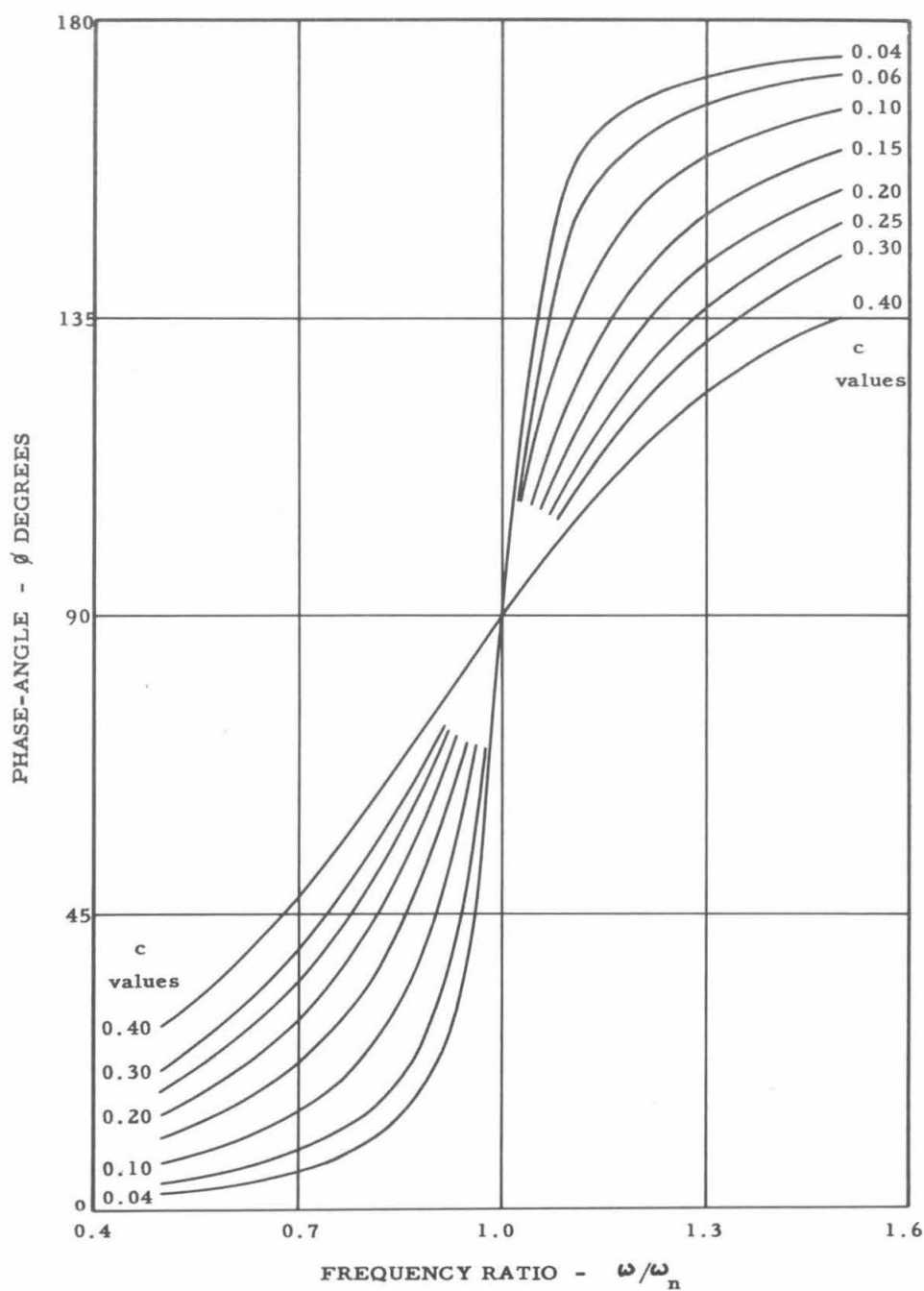


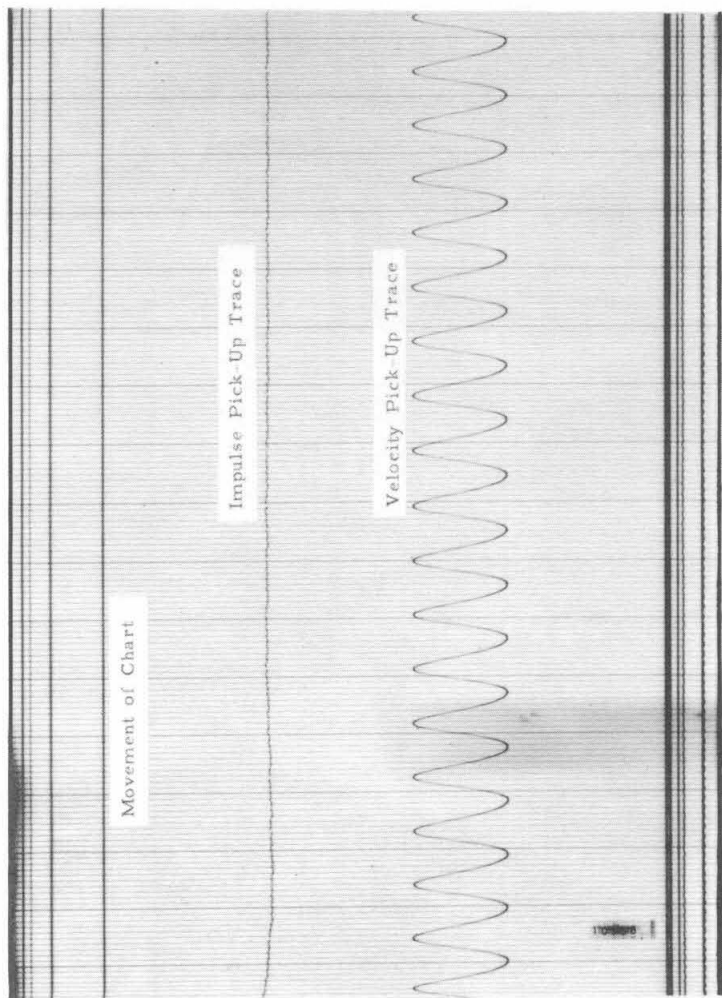
Fig. 1.9

RELATIONSHIP BETWEEN FREQUENCY RATIO AND PHASE-ANGLE
FOR A LINEAR VIBRATING SYSTEM WITH VARIOUS DAMPING
FACTOR RATIOS.

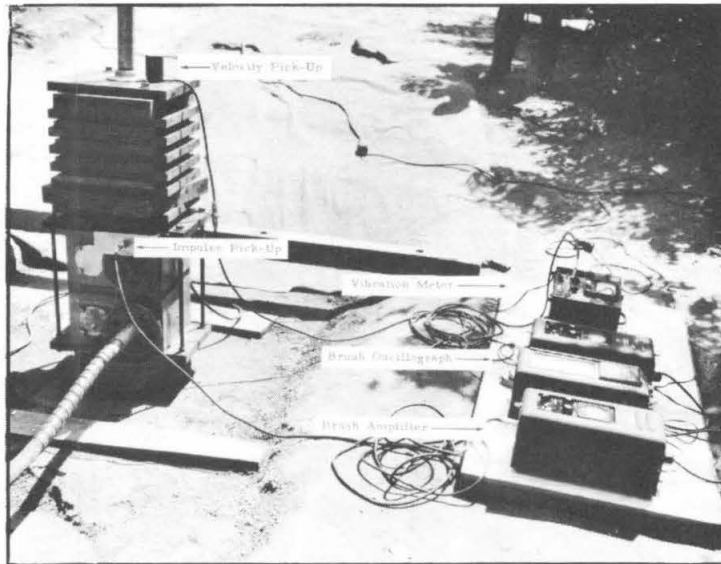
exactly in line with the steel screw when this was at the uppermost position of its circular path. The output of this pick-up was fed through an amplifier to the moving chart of a recording oscillograph, upon which was simultaneously recorded the output of a velocity pick-up measuring the displacements of the vibrator.

At first Brush recording equipment was used, but it was found that the time length of the pulse from the impulse generator was too short (of the order of 0.0005 seconds), to cause the recording pens to be actuated. Due to their inertia, the pens of the Brush oscillograph are apparently insensitive to frequencies greater than about 100 cycles per second. A Miller oscillograph was then brought into use, being an instrument recording the movement of a spot of light on a photographically sensitized chart. The light is reflected from a mirror attached to a galvanometer which vibrates in accord with the input to the oscillograph from an external source of vibration, such as the impulse pick-up or the velocity pick-up. Having almost negligible inertias, the galvanometers are responsive to extremely high values of frequency. The instrument used contained twelve such galvanometers, hence it was possible to record side-by-side the outputs of the impulse pick-up and the velocity pick-up.

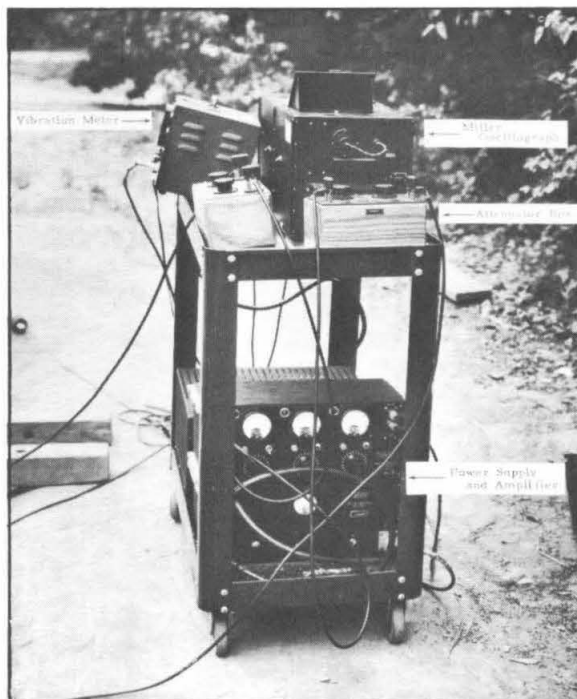
The complete assembly of measuring instruments thus consisted of a Miller oscillograph recording the time-displacement relationship of the vibrator simultaneous with the time-position relationship of the steel screw; and the Consolidated Vibration meter recording the value of the displacements during the tests. A comparison of the two assemblies of electronic measuring equipment is given on Plate 1.4. Photograph 1.4 (A) shows a velocity pick-up connected to the vibration meter, from which connection is made through an amplifier to the Brush oscillograph. The impulse pick-up is connected through a second amplifier to the second channel of the Brush oscillograph. Photograph 1.4 (B) shows the Miller oscillograph assembly, in which the outputs from the one velocity pick-up and from the impulse pick-up were fed through attenuator boxes, to an amplifier, and from there to two of the channels of the Miller oscillograph. The attenuator boxes were necessary to reduce the peak voltages, being generated by the pick-ups, which would otherwise have overloaded the amplifier. A second velocity pick-up shown on Plate 1.2 which illustrates the mounting of the



A Portion of the Miller Oscillograph Chart for the Resonant
Condition in Test I11-46.



(A) Assembly of Brush Instruments in early Attempts to Measure Phase Angles.



(B) Assembly of Miller Instruments in later Attempts to Measure Phase Angles.

various pick-ups, was connected directly to the vibration meter. Plate 1.3 shows a typical portion of the chart from the Miller oscillograph. During the tests, the spot of light at the moment of the pulse from the impulse pick-up moved so rapidly that it could not be recorded on the sensitized paper, the position of the pulse thereby being indicated on the chart by a blank space in the trace. The movement of the whole vibrator is shown by the sinusoidal wave-form.

From the chart the phase-angle was readily calculated. Using a travelling microscope with a vernier scale giving dimensions to 0.001 inch, the following measurements were made:

- (a) Rate of travel of chart (note that each vertical line on the chart represents 0.01 seconds);
- (b) Wave-length of the motion, which, knowing the rate of travel of the chart, enabled the frequency of vibration to be accurately established;
- (c) Distance between the position of the screw and the position of the vibrator at the lowest point in its vibratory motion. Since the screw was set in line with the fixed eccentric weights on the Lazan, knowledge of the angular setting between the fixed and movable eccentrics enabled the direction of the force corresponding to the position of the screw to be computed.

The procedure used to determine the phase angles is shown in Table 1.6. Referring to Fig. 1.10 which shows the basis of this procedure, it is seen that the motion of the vibrator is represented in angular form, in the manner used to derive the equations for a sinusoidal vibrating motion of which the most widely known example is Simple Harmonic Motion.⁽⁶⁾ In this instance, 0° is taken as representing the lowest position of the vibrator in the cycle; at 90° the vibrator is moving upwards through the equilibrium position with maximum velocity; at 180° the highest position in the cycle is reached; and at 270° the vibrator is moving downwards through the equilibrium position. Fig. 1.10 (b) shows the screw at the moment when its position is recorded on the oscillograph record. It is then in the 180° position, but due to the angle between the fixed and movable eccentrics on the shaft of the oscillator, the direction of the force is $(180-\theta)/2$ degrees behind this position. From Fig. 1.10 (c) it is seen that, with the oscillograph chart moving from right to left, the position of the screw is re-

recorded some time before the vibrator in its lowest position. If l is the distance between the recorded position of the screw and the lowest position of the vibrator, and L is the wave-length of the motion, then:

Angular position of the screw when vibrator is at 0° is:

$$180^\circ + \left(\frac{l}{L} \times 360^\circ\right)$$

Note that 180° enters the above equation since the position of the screw is recorded when it is at the 180° mark.

The angular position of the dynamic force when the vibrator is at 0° is then:

$$180^\circ + \left(\frac{l}{L} \times 360^\circ\right) - \left(\frac{180^\circ - \theta}{2}\right)$$

The phase angle between the dynamic force and the motion of the vibrator is thus:

$$180 + \left(\frac{l}{L} \times 360\right) - \left(\frac{180 - \theta}{2}\right) - 0 \text{ degrees}$$

$$\text{or, } \phi_1 = 90 + \left(\frac{l}{L} \times 360\right) + \frac{\theta}{2} \text{ degrees} \quad (1.6)$$

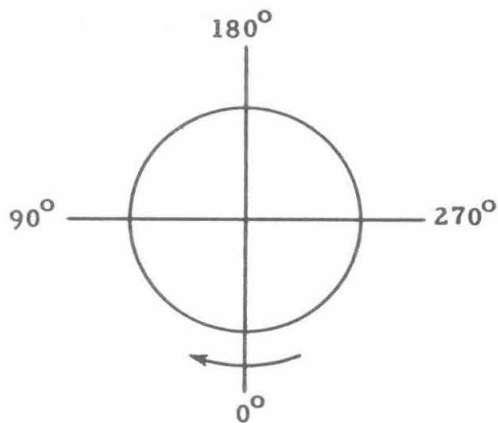
The computation procedure is then as follows:

(a) The wave-length (L), lag of the velocity pick-up (1), and rate of travel (R) of the chart are measured as previously outlined, and entered in columns (2), (3), and (7), respectively, of Table 1.6.

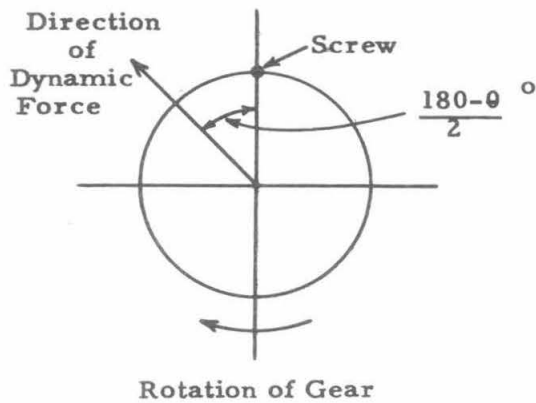
(b) The angular settings, θ , of the Lazan eccentrics, are entered in column (5), and the apparent phase angle ϕ_1 is computed from equation (1.6).

(c) The phase-angles introduced by the measuring instruments are then entered in column (10). As can be seen, these values are quite considerable, and are effected by the frequency of operation and by the amount of displacement of the pickups. Very careful calibration tests were conducted over a wide range of frequencies and displacements, the data from which were plotted to give curves relating instrument phase-angle to the frequency and displacement. These last values are entered in columns (8) and (9) respectively, and the phase-angle corrections then determined from the calibration curves and entered in column (10) giving the values ϕ_2 .

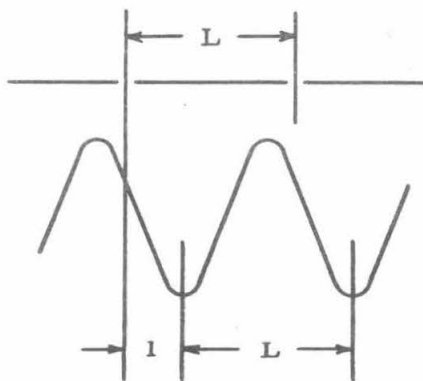
(d) The true corrected phase-angle between the dynamic force and the motion of the vibrator is then given by the equation:



(a) Angular representation of motion of vibrator.



(b) Position of force vector at instant when position of screw is recorded on oscillograph chart.



(c) Traces given by impulse pick-up and by velocity pick-up.

Fig. 1.10 BASIC DIAGRAMS USED TO SET-UP PHASE-ANGLE ANALYSIS EQUATIONS.

TABLE 1.6

CALCULATION OF PHASE ANGLES, TEST L11-46

Measurements Taken from Miller Oscillograph Record

(1) Record No.	(2) Wave Length	(3) Lag of Velocity Pick-Up	(4) $360 \times \frac{l}{L}$	(5) Angular Setting of Eccentrics	(6) Apparent Phase Angle	(7) Rate of Travel of Chart	(8) Frequency of Vibration R/L	(9) Displace- ment of Vibrator peak-to-peak mils.	(10) Phase Angle Correc- tion	(11) Corrected Phase Angle $\phi_1 - \phi_2$
	L in.	1 in.	degrees	θ degrees	ϕ_1 degrees	R in./sec.	c.p.s.		ϕ_2 degrees	ϕ degrees
10953	0.5312	0.123	83.4	141.5	244.2	4.880	9.19	37.5	237.8	6.4
10954	0.5020	0.140	100.4	141.5	261.2	4.903	9.77	61	252.0	9.2
10955	0.4672	0.139	107.1	141.5	267.9	4.869	10.42	87	260.3	7.6
10956	0.4590	0.233	182.7	141.5	343.5	4.894	10.66	280	258.7	84.8
10957	0.4196	0.257	220.5	141.5	381.3	4.765	11.36	295	276.1	105.2
10958	0.4061	0.266	235.8	141.5	396.6	4.743	11.71	295	281.2	115.4

$$\phi = \phi_1 - \phi_2 \quad \text{degrees}$$

The values of ϕ are entered in column (11), and are plotted against the corresponding frequencies of vibration to give the curve shown in Fig. 1.11.

From Fig. 1.11 it is possible to determine the resonant frequency for this test, and then to calculate values of the frequency ratio corresponding to the frequencies in column (8). For test L11-46, the resonant frequency as determined in this way is 10.7 c.p.s. which is identical to the value obtained for this test using the displacement analysis method. A plot of frequency ratio vs. phase angle results in the curve shown in Fig. 1.12, which, when compared with the theoretical curves shown in Fig. 1.9 enables values of the damping factor ratio to be determined. The dynamic amplification and contact pressures are then computed in the manner shown in Table 1.5.

1.10 Test Results

Considerable difficulty was experienced in properly investigating the various parameters under consideration, due to the limitations of the equipment. Frequently the data appeared to conform to a specific pattern, or showed a trend towards a definite type of relationship, but when tests were planned to establish, or otherwise, these patterns and relationships, they could not be carried to the desired limits. The investigation of the effect of F_o/W ratio is a particularly notable example of this state of affairs, as already mentioned in section 1.6 of this chapter. Nevertheless, much useful data has been obtained, and in general these data have been found to conform to the theories and hypotheses formulated during the earlier work on less cohesive soils.

During the progression of the test program a marked instability in the resonant frequency was observed. By this is not meant the tendency for excessive tilting and lateral motion that was frequently observed at the resonant frequency, but the ease by which the latter could be induced by the application of slight external disturbances. Thus, it was noticeable that when the displacements were showing a slight rise just before the true resonance was reached, say at a frequency ratio of about 0.9, a resonant condition could be induced by such means as a slight increase of the force being exerted on the guide rod used to control the amount of lateral motion of the vibrator. In a few cases where a cycle of frequencies was run through more than once

in a particular test, the resonant frequencies in the successive cycles were markedly different. In this respect attention is drawn to the data shown in Table 1.1 for Tests L11-3 L11-10, L11-11, L11-12, L11-13, and L11-17.

1.10.1 Effect of the Soil and Moisture Content

The amount of compaction obtained in the tests was found to be considerably effected by the moisture content of the soil. Series of tests were run under three sets of planned conditions, one of which was that the ratio F_o/W should be unity. Although this was not precisely achieved, within each set of conditions the value of the ratio was essentially constant. The planned conditions were as follows with the range and average values of the F_o/W ratio actually obtained being shown in each case:

(1) Dead weight, 495 pounds.

Base plate area, 148 sq. in.

F_o/W ratio:	Maximum:	0.93
	Minimum:	0.92
	Average:	0.925

(2) Dead weight, 662 pounds.

Base plate area, 148 sq. in.

F_o/W ratio:	Maximum:	1.041
	Minimum:	0.85
	Average:	0.953

(3) Dead weight, 1180 pounds.

Base plate area, 148 sq. in.

F_o/W ratio:	Maximum:	0.766
	Minimum:	0.621
	Average:	0.684

The tests conducted under these conditions are shown in Table 1.7, and the results are plotted on Fig. 1.13. Certain of the tests listed in Table 1.7 were not used to construct Fig. 1.13 due to factors listed in the 'remarks' column of the Table.

It will be observed that the moisture-density relationships follow the normal

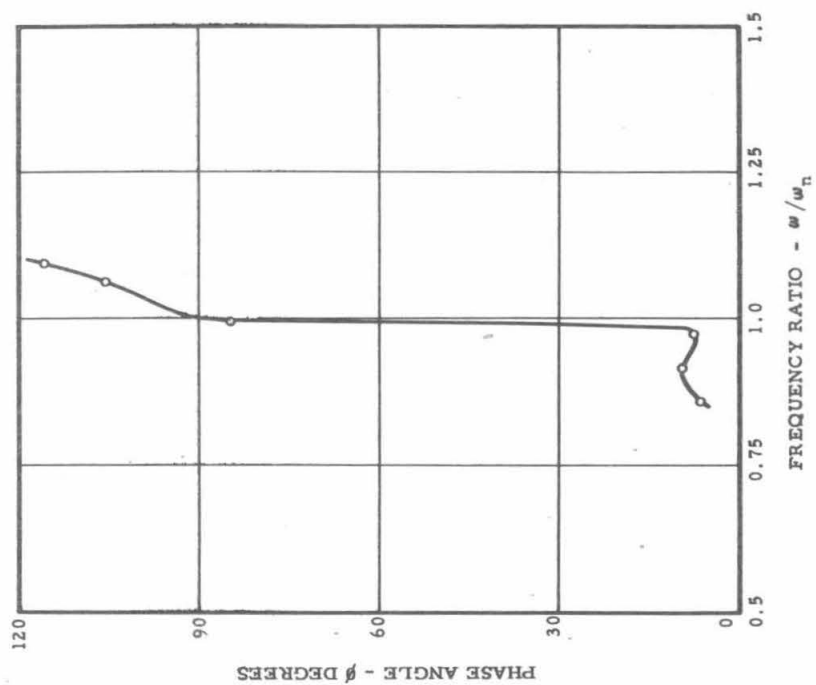


Fig. 1.12 RELATIONSHIP BETWEEN FREQUENCY RATIO AND PHASE ANGLE, TEST L11-46

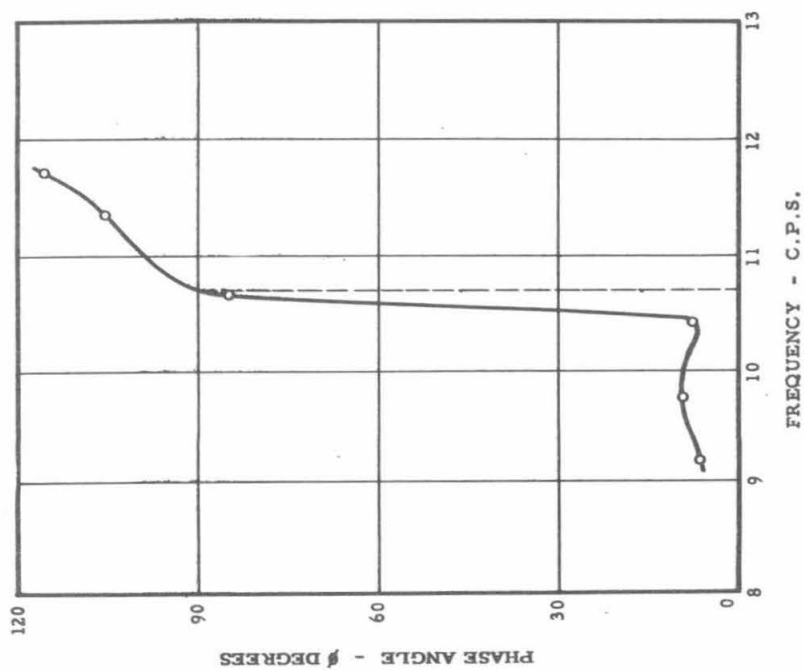


Fig. 1.11 RELATIONSHIP BETWEEN FREQUENCY OF VIBRATION AND PHASE ANGLE BETWEEN APPLIED DYNAMIC FORCE AND VIBRATOR MOTION, TEST L11-46

TABLE 1.7

TESTS CONDUCTED TO INVESTIGATE MOISTURE-DENSITY RELATIONSHIP

Soil - CL-Type from Reseda

Test No.	Dead Weight W lb.	Remarks
L11-3	495	Moisture content of soil varied excessively
L11-3A	do.	do.
L11-8	do	
L11-11	do	Vibrator subject to excessive tilting and lateral motion
L11-17	do	
L11-9	662	
L11-12	do.	Vibrator subject to excessive tilting and lateral motion
L11-18	do.	
L11-23	do.	
L11-24	do.	Vibrator at frequency greater than resonance
L11-25	do.	do.
L11-35	do.	
L11-35A	do.	
L11-37	do	Vibrator subject to excessive tilting
L11-39	do.	Vibrator subject to excessive tilting and lateral motion
L11-42	do.	
L11-44	do.	
L11-44A	do.	Vibrator subject to excessive tilting
L11-36	1180	
L11-38	do.	Vibrator subject to excessive tilting and lateral motion
L11-38A	do.	
L11-40	do.	
L11-43	do.	
L11-45	do.	
L11-47	do.	Soil prepared at high initial density; vibrator operated for long period of time over wide frequency range in search of a "harmonic resonance"
L11-47A	do.	

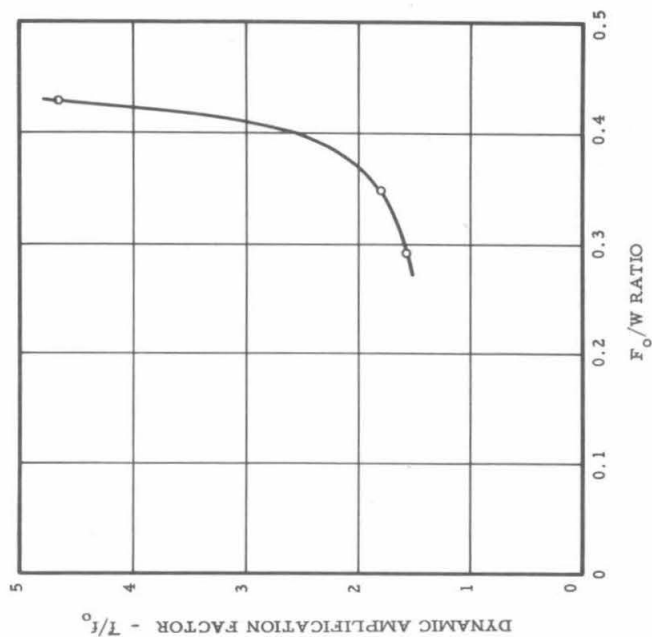


Fig. 1.14 INCREASE IN DYNAMIC AMPLIFICATION FACTOR WITH INCREASE IN F_o/W RATIO, FROM TESTS BY PAUW.

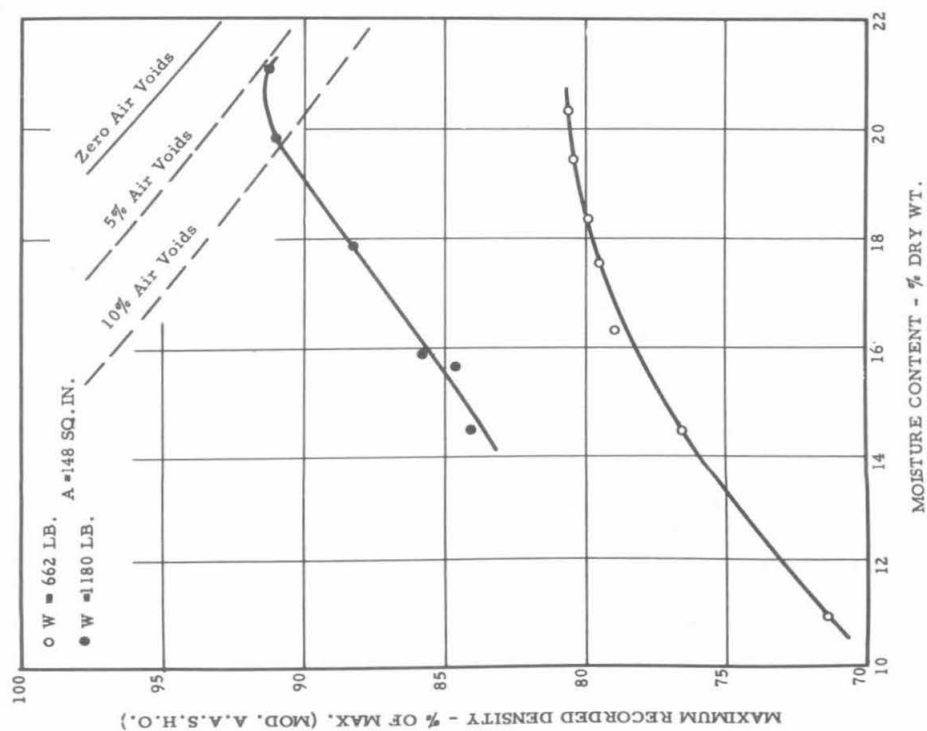


Fig. 1.13 MOISTURE - DENSITY RELATIONSHIPS IN TESTS L11.

pattern of rising density with increasing moisture content until a peak value is reached. The optimum value for the tests utilizing a dead weight of 662 pounds was about 21%; and for those utilizing a dead weight of 1180 pounds it was somewhat less, at about 20.6%. These optimum moisture contents are relatively high and no tests were possible in the time available to determine the relationship at moisture contents higher than the optimum values. However, where the higher dead weight was used, it appears from the proximity of the peak of the curve to the zero air void line that there must be a comparatively rapid decrease in density as the moisture content exceeds about 22%.

One aspect considered of significance during the progression of the test program was that the then uncompleted curves appeared to peak at the plastic limit of the soil, a fact confirmed when the program was completed and Fig. 1.13 was constructed. This is now felt to be more of a coincidence than a criterion for determining optimum field operating conditions. It appears far more likely that with the availability of heavier equipment, and attendant greater contact pressures, the optimum moisture content will be closer to the value given by the modified A.A.S.H.O laboratory compaction test. Indeed, if densities approaching the laboratory maximum are to be obtained with this particular soil, the optimum moisture content for any heavier vibratory equipment must be less than the values indicated on Fig. 1.13, due to the physical limitations presented by the moisture-density relationship with zero air voids in the soil.

A feature related to the amount of moisture present in the soil was the formation of a hard crust at relatively low moisture contents. This was also noticed with the less cohesive soils. With the Reseda CL soil at moisture contents less than about 16%, a "cake" of soil up to 1 1/2 inches in thickness adhered to the vibrator base-plate, and a hard crust up to about 2 inches in thickness was formed on the surface of the soil beneath the base-plate. Beneath this hard crust there was within a distance of two to three inches, a very rapid decrease in the density of the soil, from the compacted state to the original loose state. On the other hand, for moisture contents exceeding about 16%, very little soil adhered to the base. This is thought to be due to the action of the vibrator drawing moisture towards the base-plate, giving rise to a lubricated condition at the steel-soil interface. In addition, at these higher

moisture contents, a crust was not formed on the soil surface, the density being quite uniform to a depth of between 6 inches and 9 inches (this depth depended on the size of base-plate and the dead-weight of the vibrator), the density then gradually decreasing, although in most cases even at a depth of 18 inches some degree of compaction was still to be found.

The effect of the moisture content of the soil on the resonant frequency of the vibrator-soil system was characterized by the complete lack of any regular pattern of the results. The absolute scatter of the data was not extremely excessive, all but two of the resonant frequencies in the tests tabulated in Table 1.7 lying between 600 and 710 R.P.M. However, within these limits the distribution of the data was quite haphazard.

1.10.2 Effect of the F_o/W Ratio

For reasons already outlined in this chapter, control over the F_o/W ratio could not be exercised sufficiently to give data enabling an optimum value of this ratio to be established or confirmed. However, on the basis of the previous work on sandy loam, it is still felt that operation at an F_o/W ratio approaching unity will give the best results. The value of such a procedure is partly attributed to the fact that for a given dead weight, a greater dynamic force, and hence greater contact pressure, will be available for compaction purposes. In addition, the work of Dr. Pauw⁽³⁾ shows that the dynamic amplification factor at resonance increases rapidly as the F_o/W ratio increases, as shown in Fig. 1.14. There is no reason to suppose that this relationship exhibited by a cohesionless soil will not also be exhibited by a cohesive soil.

1.10.3 Effect of Dead Weight, Dynamic Force, and Contact Pressure

These parameters are so interrelated that it is impossible to consider the effect of any one separately, except possibly contact pressure. To consider any one separately, all other parameters in the tests must be maintained constant. This is not possible. If for instance dynamic force and base-plate area are fixed and the dead weight is varied, then the F_o/W ratios and the contact pressures also vary. It is seen in fact that only the soil moisture content can be varied without effecting the remaining parameters. Furthermore, it can be seen that all of these remaining

parameters can eventually be considered in terms of contact pressures, although this is only partially the case for the F_0/W ratio.

Effect on Resonant Frequency

The impossibility of taking each of these parameters separately is, of course, only true when considering their effect on the density of the soil. The resonant frequency of the vibrator soil mass is known to be effected by the mass of the vibrator and the applied dynamic force. In previous work the resonant frequency has decreased as the dynamic force and dead weight have increased. In the tests on the Reseda CL soil, the resonant frequencies were haphazardly distributed, and no such relationship could be considered as established. It is significant however that over the whole moisture range, the tests involving the two most frequently used dead weights, 662 pounds and 1180 pounds, show average resonant frequencies which for all practical purposes are equal.

For W 662 pounds, average resonance 663 R.P.M.

For W 1180 pounds, average resonance 670 R.P.M.

The reason for this is probably that the cohesiveness of the CL-type soil is such that a larger total mass is being vibrated. Hence, the mass of the vibrator is very small compared with the whole vibrating mass, so that the difference between the two above dead weights is small compared with the whole. This is illustrated in Table 1.8 which presents data from the tests in which it was possible to calculate the total vibrating mass. The spring constants shown in column (2) are those obtained during the displacement analysis method computations for the dynamic amplification factors in these tests, the total vibrating mass being related to the spring constant according to the fundamental equation:

$$m_t = \frac{k}{\omega_n^2}$$

Effect on Soil Density

No definite relationship between dead weight, and therefore also dead weight contact pressure, and resulting soil density can be established from the tests on the Reseda CL soil. The data, when plotted to show the relationship between these

TABLE 1.8

TOTAL VIBRATING MASS IN TESTS L11-42 TO L11-47

$$m_t = \frac{k}{\omega_n^2}$$

(1) Test No.	(2) Spring Constant at Resonance k	(3) Resonant Frequency	(4) Resonant Frequency ω_n	(5) Total Vibrating Mass m_t	(6) Dead Weight of Vibrator W	(7) Mass of Vibrator m_v	(8) Mass Ratio $\frac{m_v}{m_t}$
	lb./in.	c.p.s.	rad./sec.	$\frac{\text{lb. sec.}^2}{\text{in.}}$	lb.	$\frac{\text{lb. sec.}^2}{\text{in.}}$	
L11-42	189,670	12.50	78.55	30.74	662	1.71	0.056
L11-43	139,825	11.16	70.13	29.43	1180	3.05	0.104
L11-44	153,570	9.99	62.78	38.96	662	1.71	0.044
L11-44A	149,070	9.96	62.59	38.05	662	1.71	0.045
L11-45	120,485	10.75	67.55	26.40	1180	3.05	0.116
L11-46	132,145	10.69	67.18	29.28	1282	3.32	0.113
L11-47	138,235	12.05	76.72	24.11	1180	3.05	0.127

variables exhibit a considerable amount of scatter from which no trends can be observed, and for which no conclusions may be drawn.

There does, however, appear to be a very definite straight-line relationship between the total nominal contact pressure and the resulting soil density in these tests. Neglecting those tests in which additional factors such as excessive tilting and lateral motion were experienced, groups of data representing three test conditions have been plotted on Fig. 1.15, Fig. 1.16 and Fig. 1.17, which clearly indicate the straight-line form of the relationship. No explanation has yet arisen to account for this relationship.

Table 1.9 summarizes the results of the calculations for contact pressures using the displacement analysis method. In columns (8) and (9) in the Table are recorded the lower and upper limits to the values of the shear strength of the soil, based on the results of direct shear tests (see Chapter 2). Those strengths in column (8) represent the lower limits, and are the cohesive strengths only, as if the frictional strength were non-existent. However, the unknown nature of the part played by friction, for which the hypothesis of non-existence was presented in section 1.7.1, has led to the calculation of shear strengths including the full effect of the coefficient of friction as determined by the direct shear tests, thus establishing an upper limit to the strength values. These are shown in column (9).

Coulomb's equation ($s = c + N \tan \phi$) has been used to determine these shear strengths, and for comparison purposes the values have been calculated at the depth where the maximum shear stress is developed in the soil, i.e. at a depth of about three-eighths of the diameter of the base plate. In Coulomb's equation, N is the normal load on the plane of maximum shear stress. At the immediate edge of the base plate, at the soil surface, the shear plane is vertical, and at this point there is no horizontal pressure in the soil. The shear strength is therefore only the cohesive strength of the soil. The maximum value of the shear strength is found directly underneath the center of the base-plate, for which position of the normal load is given by:

$$N = \sigma_3 + \frac{(\sigma_1 - \sigma_3)}{2} = \frac{\sigma_1 + \sigma_3}{2} \quad (1.7)$$

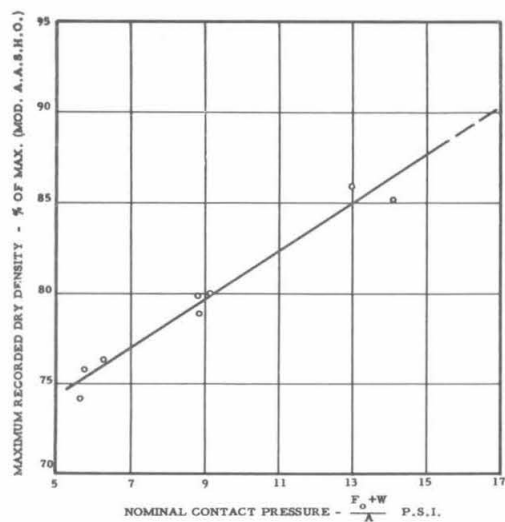


Fig. 1.15 RELATIONSHIP BETWEEN NOMINAL CONTACT PRESSURE AND
MAXIMUM RECORDED DRY DENSITY FOR A MOISTURE CONTENT
OF 16% TO 17%, AND BASE AREA OF 148 SQ. IN., TESTS L11.

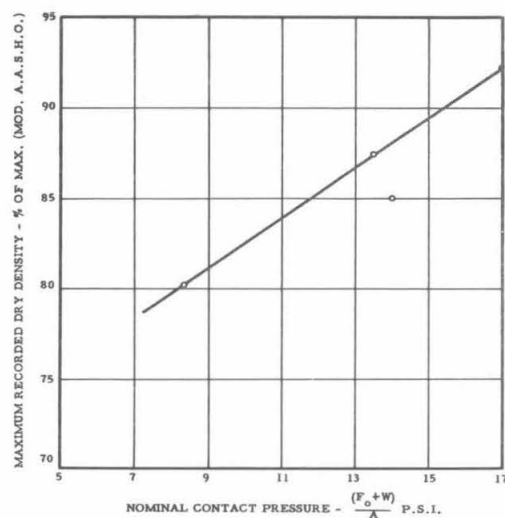


Fig. 1.16 RELATIONSHIP BETWEEN NOMINAL CONTACT PRESSURE AND
MAXIMUM RECORDED DRY DENSITY FOR A MOISTURE CONTENT
OF 20% AND A BASE AREA OF 74 SQ. IN., TESTS L11.

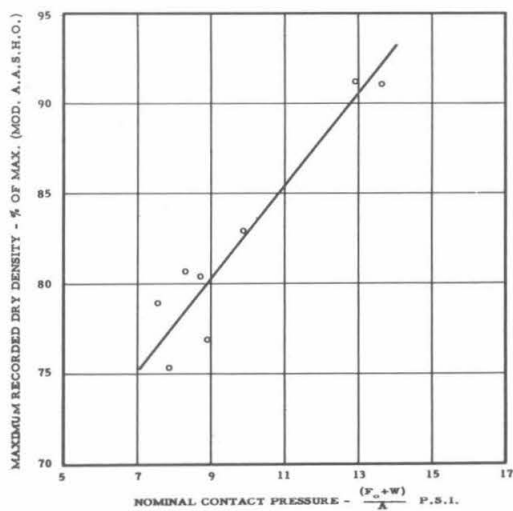


Fig. 1.17 RELATIONSHIP BETWEEN NOMINAL CONTACT PRESSURE AND
MAXIMUM RECORDED DRY DENSITY FOR A MOISTURE CONTENT
OF 20% AND A BASE AREA OF 148 SQ. IN., TESTS L11.

TABLE 1.9
DYNAMIC AMPLIFICATION FACTORS AND CONTACT PRESSURES
FOR RESONANT CONDITIONS IN TESTS L11-42 TO L11-47

Displacement Analysis Method

(1) Test No.	(2) Dead Weight	(3) Moisture Content	(4) Damping Factor Ratio	(5) Spring Constant	(6) Dynamic Amplifica- tion Factor	(7) Dynamic Contact Pressure	(8) Lower Limit of Shear Strength	(9) Upper Limit of Shear Strength	(10) Maximum Shear Stress in Soil	(11) Maximum Recorded Dry Density
	W lb.	w % dry wt.		k lb./in.	\bar{F}/F_o	\bar{T} p.s.i.	p.s.i.	p.s.i.	p.s.i.	% of max.
L11-42	662	15	0.01	189,670	48.35	185.6	8.54	54.3	59.1	76.5
L11-43	1180	15	0.02	139,825	25.00	134.6	8.54	41.7	42.8	84.0
L11-44	662	16	0.01	153,570	50.36	219.5	9.72	61.9	69.8	78.9
L11-44A	662	16	0.01	149,070	49.93	216.3	9.72	61.1	68.8	79.9
L11-45	1180	21	0.02	120,485	24.87	126.2	5.20	18.6	40.3	91.2
L11-46	1282	22	0.02	132,145	25.00	125.0	4.16	14.1	39.8	91.1
L11-47	1180	20	0.02	138,235	25.00	158.8	6.59	27.7	50.5	94.7

where σ_1 = vertical pressure

and σ_3 = horizontal pressure.

The value to accord σ_3 is problematical. It may be taken as lying between the lower limit of zero and the upper limit given by the existence of full passive resistance in the soil, although such an upper limit is considered as quite unrealistic. The extent to which horizontal pressures are developed is a function of Poissons Ratio, which for elastic materials is always between zero and 0.5. For points directly below the load, the pressures are a maximum when Poissons ratio has its minimum value of zero, and so for the establishment of upper limits to the shear strengths, this value has been assumed. With this assumption, and using the Boussinesq equations for the distribution of stresses in a soil mass, it has been shown that at a given depth below the surface the horizontal soil pressures are one-sixth of the vertical pressures. It is felt that the Boussinesq values are as reasonable as might be given by any other assumptions.

Consequently, equation (1.7) becomes:

$$\begin{aligned} N &= \frac{\sigma_1 + 0.167 \sigma_1}{2} \\ &= \frac{1.167 \sigma_1}{2} \end{aligned}$$

To determine the shear strengths in column (9), the surface constant pressure \bar{f} is substituted for σ_1 , and the Boussinesq coefficient 0.8 introduced to give the vertical pressure at a depth of three-eighths of the diameter of the base-plate. The upper limits of the shear strengths are then given by:

$$\begin{aligned} s &= c + 0.8 \frac{1.167 \bar{f}}{2} \tan \phi \\ \text{or, } s &= c + 0.467 \bar{f} \tan \phi \end{aligned} \quad (1.8)$$

It can be seen that the maximum shear stress (\bar{f}/\bar{N}) in all cases exceeds the theoretical maximum values for the shear strength of the soil as shown in column

(9), and certainly exceeds by far the values of cohesive strength. Nevertheless, in four of the seven tests, those conducted on soil with a moisture content of 16% or less, satisfactory densities were not obtained. The probable reason for this is that in each of these four tests a crust of hard dense soil was found to a depth of about 2 inches at the soil surface, and extending over an area somewhat larger than the diameter of the base-plate (due to the lateral motion, however small, that inevitably occurred during the tests). This crust is thought to have given some support to the vibrator, thereby reducing the pressures in the soil below the crust. At the higher moisture contents, this condition was not observed, and satisfactory densities were obtained. It should also be pointed out that the excess of shear stress over maximum shear strength is much greater in the tests at the higher moisture contents than in those at the lower moisture contents. Note that the values of cohesion and internal friction used to calculate the shear strengths were determined from samples of disturbed soil compacted to a density of about 90% of maximum. It was anticipated that if shear stresses could be applied in excess of the shear strengths given on this basis, then the resulting densities would exceed 90% of maximum. This did occur.

1.10.4 Effect of the Diameter of the Base Plate

At the outset, base-plates of 13-3/4 inches and 15-3/4 inches diameter were available, and were used to support the vibrator mass on the soil surface. As it became necessary to increase contact pressures plates 9-3/4 inches in diameter were introduced, although this step was taken only as a last resort when the use of two Lazan oscillators did not appear to be raising the contact pressures to sufficiently high values.

Undoubtedly the use of these smaller base-plates resulted in higher contact pressures and much higher soil densities, see Test L11-27, Table 1.1, but the question was raised as to whether or not this increase in density was partially due to a "size-effect." The same question concerning the possible existence of a size-effect had been posed before the introduction of these plates, and had caused the delay in taking this step to the point when it appeared unavoidable. Consequently, at the first possible moment, tests were conducted to determine whether or not a size-effect existed. A series of three tests was conducted using the 9-3/4 inch (1/2 sq. ft.), 13-3/4 inch

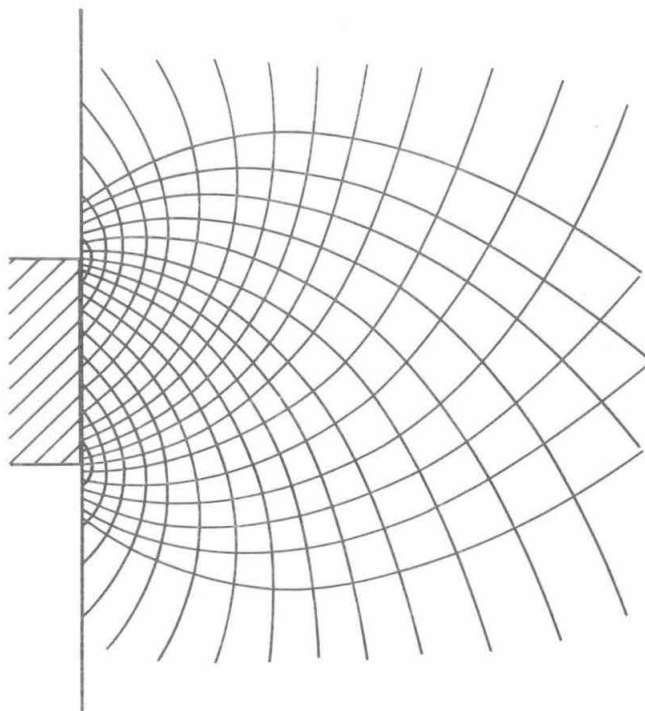


Fig. 1.19 SLIP LINES FOR A LOAD ACTING ON
THE EDGE OF A METAL PLATE,
FROM "PLASTICITY"
BY A. NADAI

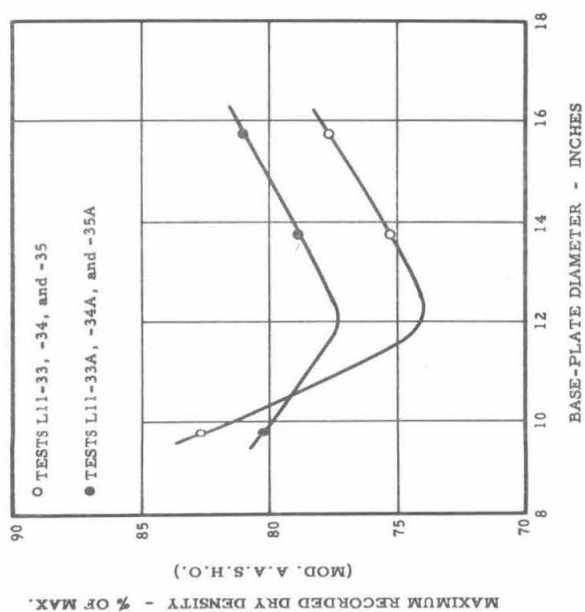


Fig. 1.18 RELATIONSHIP BETWEEN BASE-PLATE DIAMETER AND
MAXIMUM DRY DENSITY, TESTS L11.

(1 sq. ft.), and 15-3/4 inch (1-1/2 sq. ft.) base plates; an F_o/W ratio of unity; and a dead weight so adjusted as to give nominal contact pressures of the same value for all the tests. The first series did not conclusively establish the relationship between the size of the base plate and the resulting soil density, so a second identical series was conducted. The data from these tests are shown in Table 1.10, and are plotted on Fig. 1.18.

TABLE 1.10

TESTS TO DETERMINE EFFECT OF SIZE OF BASE PLATE ON
DENSITY OF SOIL

(1) Test No.	(2) Base Plate Diameter	(3) Base Plate Area	(4) Dead Weight	(5) Dead Weight Contact Pressure	(6) Maximum Recorded Soil Density
	in.	sq.in.	lb.	p.s.i.	% of max.
L11-32	9-3/4	74	295	3.99	82.7
L11-33	13-3/4	148	589	3.98	75.3
L11-34	15-3/4	193	769	3.98	77.7
L11-32A	9-3/4	74	295	3.99	80.2
L11-33A	13-3/4	148	589	3.98	78.9
L11-34A	15-3/4	193	769	3.98	80.9

It was found that a similar relationship was established by each series of tests. In both cases a definite size-effect was apparent, from which it appeared that use of a plate of about 12 inches in diameter would result in densities lower than those obtained with other base-plate sizes. A rapid increase in density was exhibited as the plate diameter became progressively less than 12 inches, and similar, though less rapid, effect for plates of progressively greater diameter than this value.

Consequently no further work was conducted with either the smallest or the largest base-plates. In addition to the question of size effect, the smallest plate

was discarded because of the unstable top-heavy situation created with the vibrator assembly, and because of the great departure it represented from the sizes of large-scale field compaction equipment that may be developed as a result of this work. It was also felt that if satisfactory densities could be achieved using the 13-3/4 inch base-plate, then at least equal results would be likely with heavier equipment on larger bases.

1.10.5 Effect of Movement of the Vibrator over the Soil Surface

One test, L11-28 (see Table 1.1), was conducted in which the vibrator was caused to travel over the soil surface, traversing five times in each direction a path 3 ft. long and one base-plate diameter in width. The resulting density was very much higher than that obtained in an identical test (L11-18) in which the vibrator was not subjected to any appreciable lateral motion.

A possible reason for this is the changing direction of shearing stress at a given point within the soil as the plate moves along the surface. This is clearly apparent if one considers the two families of curves representing the trajectories of maximum shear (and consequently the slip lines) beneath a loaded plate, as shown in Fig. 1.19.⁽⁷⁾ The action on an element of soil due the loaded plate passing along the surface may be compared to the "wiping action" usually attributed to sheepfoot rollers.

If the above concept is accepted, it leads to the suggestion that a single eccentric rotating weight on the oscillator may be more effective in producing compaction than the two eccentrics with laterally balanced forces as used in these tests, and that several passes may be more effective than static vibration.

1.11 A Practical Comparison of the Methods of Displacement Analysis and Phase-Angle Analysis

In considering the usefulness of the displacement and phase-angle analyses, it must be pointed out that no specific degree of accuracy can be assured from the measurements made in the Lazan tests L11. In fact, in the vicinity of resonant frequency, there is a definite possibility of large errors being present. This is particularly the case when using the displacement analysis method. The value of the damping factor ratio at resonance is completely dependent on the manner in which the curve of frequency ratio vs. amplitude ratio is plotted as the frequency ratio approaches unity.

A striking example of this is shown by Test L11-47, the appropriate curve for which is shown superimposed upon the theoretical curves in Fig. 1.4. The curve as drawn corresponds to a damping factor ratio of 0.02 as the frequency ratio approaches unity. However, a curve corresponding to a damping factor ratio of 0.04 may also be fitted to the plotted points of the test data without causing any greater distortion than is given by the accepted curve. Since at resonance the calculated values of the spring constant, effective dynamic force, and contact pressure are inversely proportional to the damping factor ratio, these values would be halved if the ratio increased from 0.02 to 0.04.

There are, however, limits within which these curves may be plotted. It will be seen that to construct a curve corresponding to a damping factor ratio of 0.06 would require an unnatural distortion, and hence the upper limit of the ratio for this test, L11-47, may be set at approximately 0.04. From practical considerations, the lower limit of the ratio may be set at approximately 0.01, for at even lower values the calculated forces and contact pressures increase at an extremely rapid rate. Consequently, with this establishment of the limits within which the values of the damping factor ratio must lie, the final results necessarily indicate the correct order of magnitude of the forces and pressures. Where there has been a choice of curves all of which appear to fit the plotted points from the test data, the one giving the least damping factor ratio has been accepted. The reason for this is that where the phase-angle analysis has been made, the ratio has been found to have a value generally the same as, or less than, the least value given by the displacement analysis method.

The phase-angle method is considered the most desirable of the two methods of analysis, but it unfortunately requires more complicated instrumentation, more carefully executed measurements during the tests, and very careful abstraction of data from the resulting oscillograph records. This is time-consuming, and introduces greater chances of error. On the other hand, with the necessary precautions, the results can be considered to give a very accurate representation of the conditions existing throughout the tests.

Instruments were assembled for the measurement of phase angles in tests

L11-42 onwards. However in the first two tests, an analysis was impossible due to a distortion of the wave-form given by the output of the velocity pick-up. This fault was corrected, but in the following two tests, light inadvertently entered the oscillograph and so darkened the sensitized paper that phase-angle measurements were again impossible. Consequently only in tests L11-45, -46, and -47 were phase-angle analyses completed. The results of these are shown in Table 1.11, and should be compared with the corresponding values given by the displacement analysis method shown in Table 1.9. Further comparison is afforded by Figs. 1.28 to 1.33 which show the relationships between the frequency ratio and the dynamic amplification factor and contact pressure for these tests as determined by both analysis methods. Figs. 1.20 to 1.27 show the same relationships for Tests L11-42 to L11-44A using only the displacement analysis.

TABLE 1.11

DYNAMIC AMPLIFICATION FACTORS AND CONTACT PRESSURES FOR
RESONANT CONDITIONS IN TESTS L11-45 TO L11-47

Phase-Angle Analysis Method

(1) Test No.	(2) Damping Factor Ratio	(3) Spring Constant k lb./in.	(4) Dynamic Amplification Factor F/F_0	(5) Dynamic Contact Pressure \bar{f} p.s.i.
L11-45	0.40	6,145	1.25	6.31
L11-46	0.01	264,285	49.96	249.8
L11-47	0.01	301,000	50.43	307.7

The results given by the analysis for Test L11-45 are most unusual and a very careful check of the data for this test does not bring to light any errors in taking measurements off the oscillograph record. It is thought that some disturbance of the

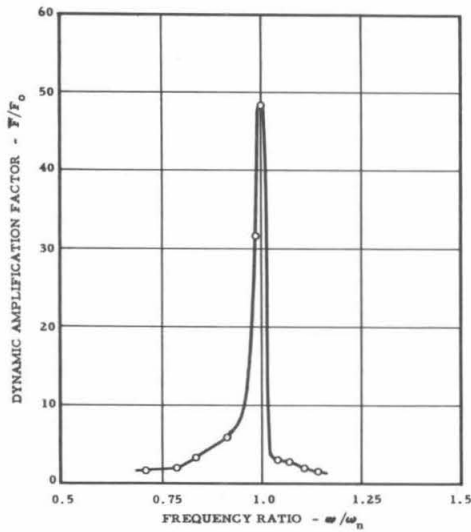


Fig. 1.20 EFFECT OF FREQUENCY OF VIBRATION ON DYNAMIC AMPLIFICATION FACTOR IN TEST L11-42, AS DETERMINED BY DISPLACEMENT ANALYSIS METHOD.

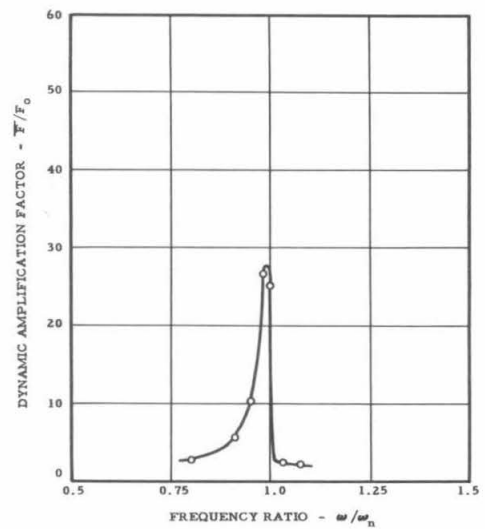


Fig. 1.21 EFFECT OF FREQUENCY OF VIBRATION ON DYNAMIC AMPLIFICATION FACTOR IN TEST L11-43, AS DETERMINED BY DISPLACEMENT ANALYSIS METHOD.

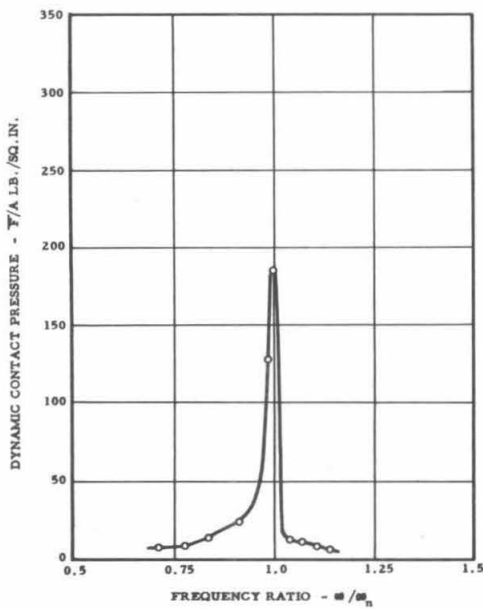


Fig. 1.22 EFFECT OF FREQUENCY OF VIBRATION ON DYNAMIC CONTACT PRESSURE IN TEST L11-42, AS DETERMINED BY DISPLACEMENT ANALYSIS METHOD.

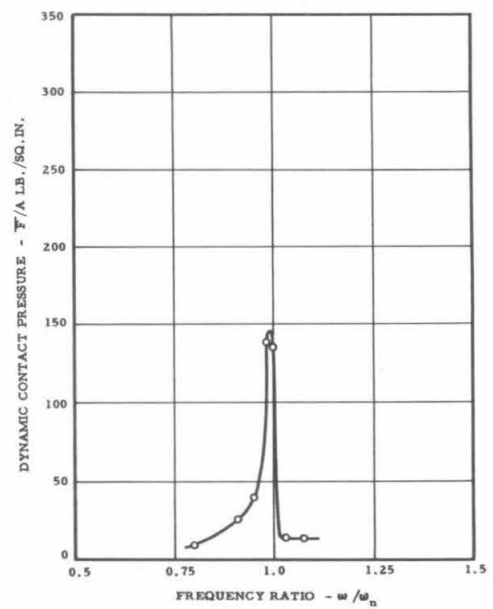


Fig. 1.23 EFFECT OF FREQUENCY OF VIBRATION ON DYNAMIC CONTACT PRESSURE IN TEST L11-43, AS DETERMINED BY DISPLACEMENT ANALYSIS METHOD.

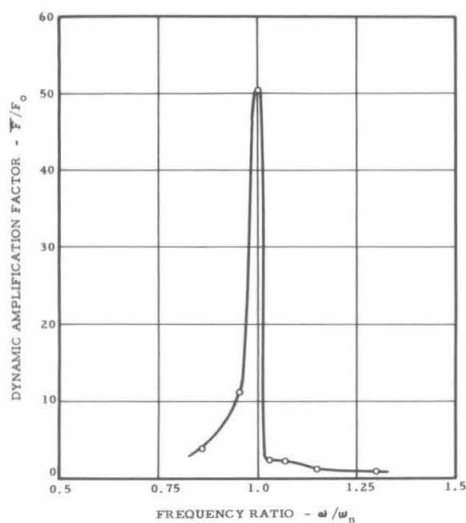


Fig. 1.24 EFFECT OF FREQUENCY OF VIBRATION ON DYNAMIC AMPLIFICATION FACTOR IN TEST L11-44, AS DETERMINED BY DISPLACEMENT ANALYSIS METHOD.

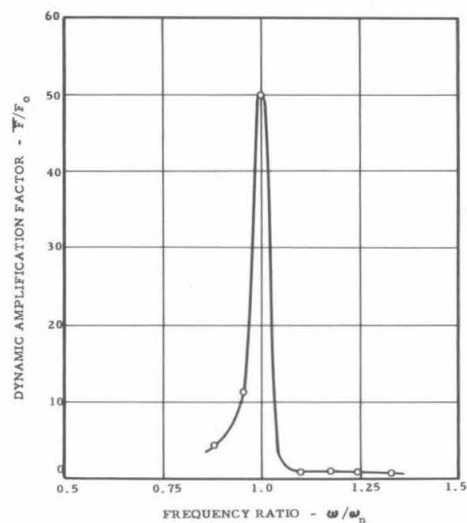


Fig. 1.25 EFFECT OF FREQUENCY OF VIBRATION ON DYNAMIC AMPLIFICATION FACTOR IN TEST L11-44A, AS DETERMINED BY THE DISPLACEMENT ANALYSIS METHOD.

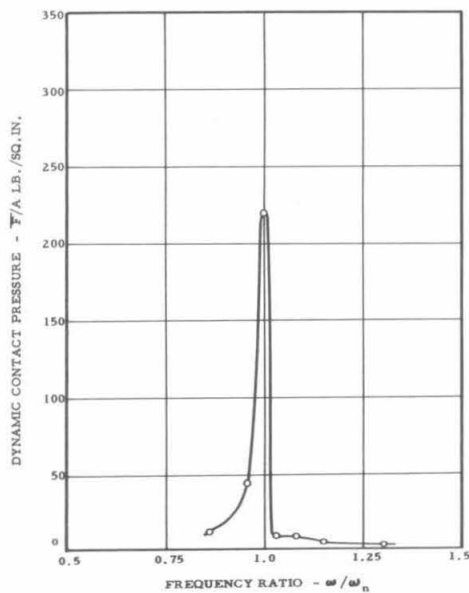


Fig. 1.26 EFFECT OF FREQUENCY OF VIBRATION ON DYNAMIC CONTACT PRESSURE IN TEST L11-44, AS DETERMINED BY DISPLACEMENT ANALYSIS METHOD.

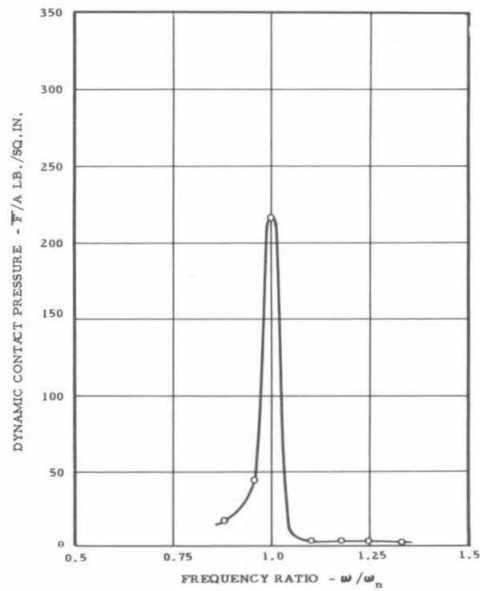


Fig. 1.27 EFFECT OF FREQUENCY OF VIBRATION ON DYNAMIC CONTACT PRESSURE IN TEST L11-44A, AS DETERMINED BY DISPLACEMENT ANALYSIS METHOD.

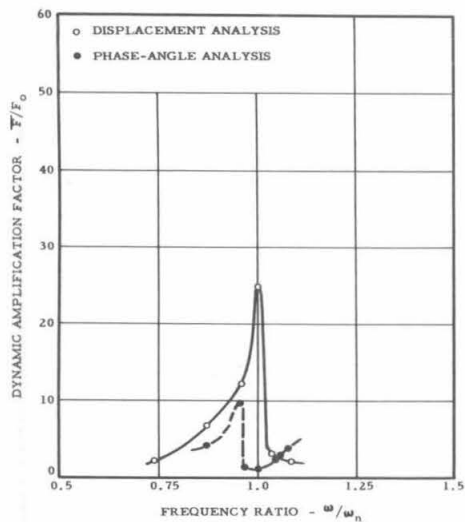


Fig. 1.28 EFFECT OF FREQUENCY OF VIBRATION ON DYNAMIC AMPLIFICATION FACTOR IN TEST L11-45, AS DETERMINED BY THE METHODS OF DISPLACEMENT ANALYSIS AND PHASE-ANGLE ANALYSIS.

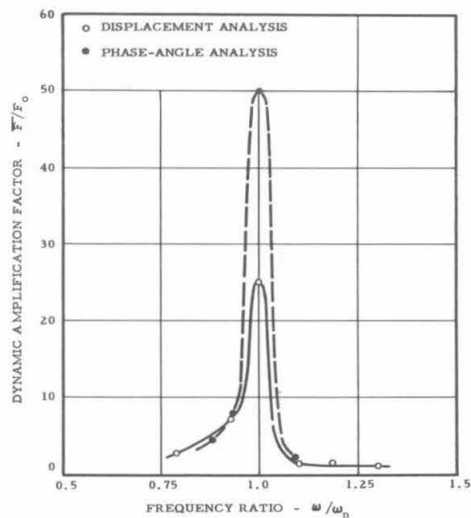


Fig. 1.29 EFFECT OF FREQUENCY OF VIBRATION ON DYNAMIC AMPLIFICATION FACTOR IN TEST L11-46, AS DETERMINED BY THE METHODS OF DISPLACEMENT ANALYSIS AND PHASE-ANGLE ANALYSIS.

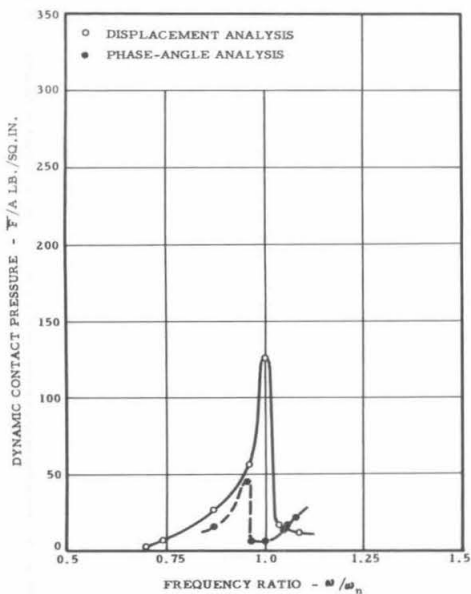


Fig. 1.30 EFFECT OF FREQUENCY OF VIBRATION ON DYNAMIC CONTACT PRESSURE IN TEST L11-45, AS DETERMINED BY THE METHODS OF DISPLACEMENT ANALYSIS AND PHASE-ANGLE ANALYSIS.

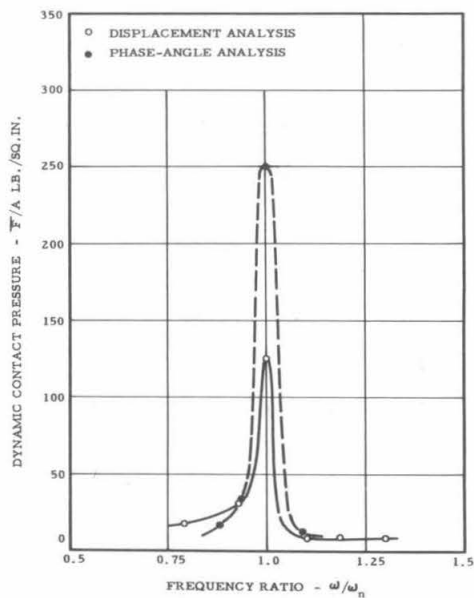


Fig. 1.31 EFFECT OF FREQUENCY OF VIBRATION ON DYNAMIC CONTACT PRESSURE IN TEST L11-46, AS DETERMINED BY THE METHODS OF DISPLACEMENT ANALYSIS AND PHASE-ANGLE ANALYSIS.

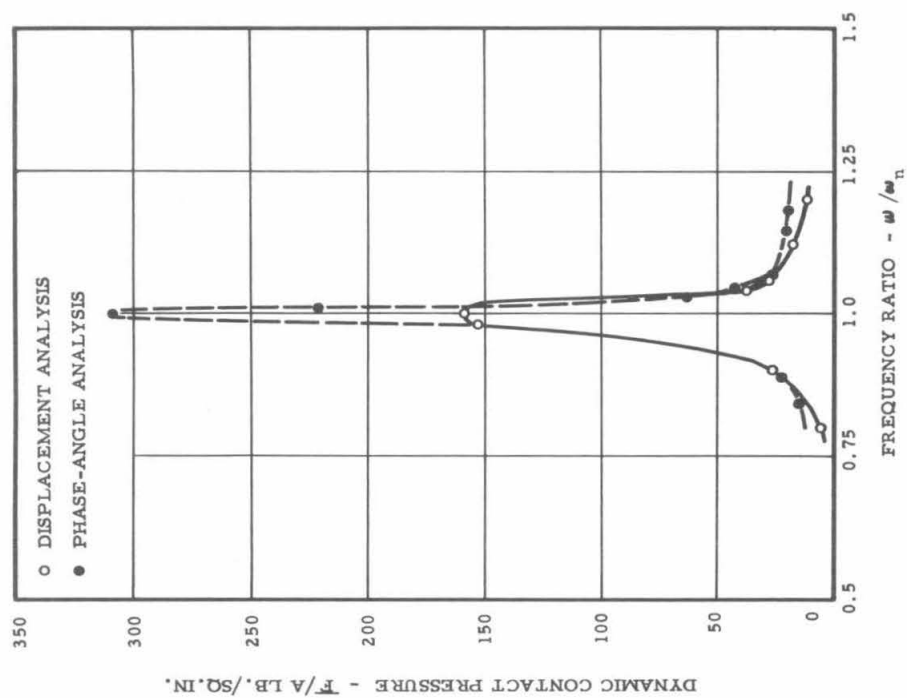


Fig. 1.32 EFFECT OF FREQUENCY OF VIBRATION ON DYNAMIC AMPLIFICATION FACTOR IN TEST L11-47, AS DETERMINED BY THE METHODS OF DISPLACEMENT ANALYSIS AND PHASE-ANGLE ANALYSIS.

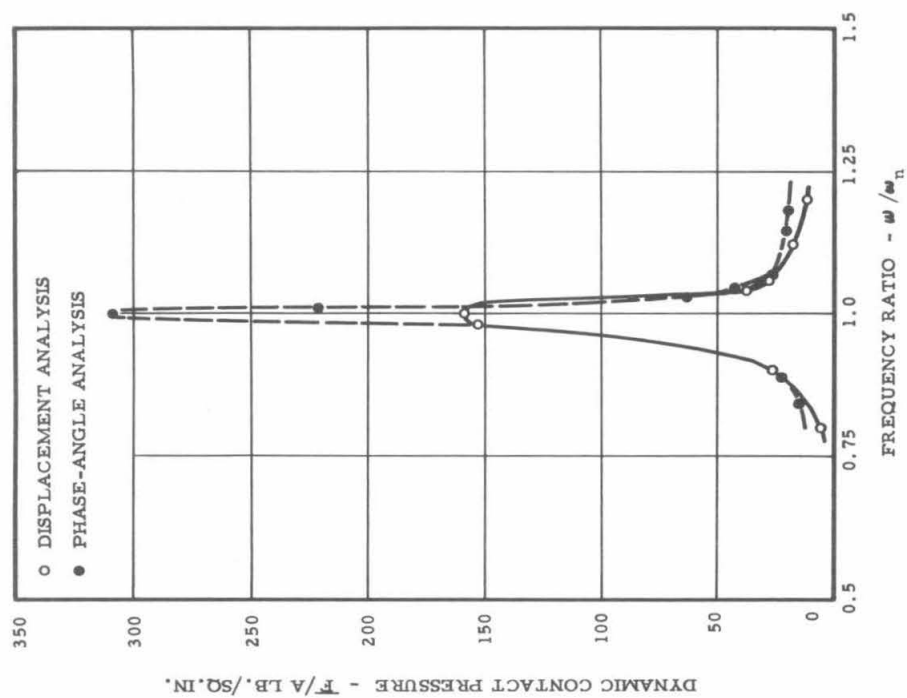


Fig. 1.33 EFFECT OF FREQUENCY OF VIBRATION ON DYNAMIC CONTACT PRESSURE IN TEST L11-47, AS DETERMINED BY THE METHODS OF DISPLACEMENT ANALYSIS AND PHASE-ANGLE ANALYSIS.

mechanism of the oscillograph occurred during the test, for the phase-angle curve follows a normal pattern as the frequencies approach resonance, but in the vicinity of the resonant frequency there is a sudden break in the curve, which gradually dies away as the frequency ratio increases beyond unity.

REFERENCES

- (1) California Institute of Technology: "An Investigation of the Compaction of Soil by Vibration," a Report on research conducted on behalf of the U. S. Army Corps of Engineers, Fort Belvoir, Virginia, March 1950.
- (2) California Institute of Technology: "Vibration-Compaction of Sand," a Report on research conducted on behalf of the U. S. Navy Bureau of Yards and Docks, U. S. Naval Civil Engineering Research and Evaluation Laboratory, Port Hueneme, California, January 1952.
- (3) Pauw, A.: "A Rational Design Procedure for Machine Foundations," a Thesis submitted to the California Institute of Technology, 1951.
- (4) Whiffin, A. C.: "The Pressures Generated in Soil by Compaction Equipment," A.S.T.M. Special Technical Publication No. 156 - Symposium on Dynamic Testing of Soils, 1953.
- (5) Bernhard, R. K. and Finelli, J.: "Pilot Studies on Soil Dynamics," A.S.T.M. Special Technical Publication No. 156 - Symposium on Dynamic Testing of Soils, 1953.
- (6) Any standard textbook of advanced mathematics of vibrations, as for example: Caunt, G. W.: "Infinitesimal Calculus," Oxford University Press, p. 153.
- (7) Nadai, A.: "Plasticity," Engineering Societies Monograph, McGraw-Hill Inc., p. 250.

CHAPTER 2

LABORATORY INVESTIGATIONS

2.1 Introduction

In order to provide information regarding the physical characteristics of the soil used in the experimental field work with the Lazan Oscillators, tests designed to determine both the shearing resistance of the compacted soil, and the shearing modulus of elasticity of the soil were made in the laboratory. It was expected that these values would help to establish a theoretical connection between the results of the field tests and the strength and rigidity of the material being tested. No attempt was made to pursue this line of investigation in great detail because of the necessity to devote the major portion of the time available for the project to completion of the field tests. The range of values obtained is, however, sufficiently extensive to make possible interesting comparisons between field compaction results and soil strength and rigidity.

2.2 Shearing Resistance of Compacted CL Soil

2.2.1 Material

The soil used in these tests was clayey-silt taken from the same supply used to prepare the pit in the work with the Lazan oscillators. The mechanical analysis is given in Chapter 1, where it is seen that 97% passes the No. 40 sieve.

2.2.2 Equipment

The tests were performed in a direct shear machine at a constant rate of displacement of approximately 0.06 inches per minute. The sample was confined in two rings each 2.41 inches inside diameter and 1 inch high. An upper box containing the upper ring was driven by a plunger actuated by a motor, but was free to rise vertically except for the resistance of the spring-applied vertical normal load. A lower box, containing the other ring, was supported on ball bearing rollers and was prevented from movement by a proving ring which recorded the shearing resistance of the soil. The line of thrust of the shearing force was along the parting line between the two rings,

which were separated by a gap of $1/32$ inch. Porous stones were placed on the upper and lower surfaces of the test specimen to permit drainage during consolidation under the normal load.

2.2.3 Procedure

Enough soil was prepared at a given moisture content to provide for at least six tests. A portion of this soil was compacted into the rings to the required density while the rings were confined in the shear boxes and the boxes were locked together.

Normal load was applied, the locking screws were released, and the motor drive was set in motion. About three minutes were required for the completion of the shearing action, deformation usually being carried to about 0.2 inches.

For each successive test at a given moisture content and initial density the applied normal loads were successively equivalent to pressures of $1/4$, $1/2$, 1, 2, 4 and 8 Kips per square foot.

2.2.4 Results

The data from each series of tests were plotted with normal load as the abscissa and shearing resistance as the ordinate. An average straight line through the resulting points was used for the determination of c and ϕ in the Coulomb equation $s = c + N \tan \phi$, where s is the shearing resistance of the soil, c is frequently called the "cohesion," N is the normal load, and ϕ is the average angle of internal friction.

Table 2.1 is a summary of the direct shear test results and Figure 2.1 shows the relations between c , ϕ and moisture content.

The following relationships may be determined from these results.

1. The "angle of friction," ϕ , decreases with an increase in moisture content.
2. At constant moisture content the "angle of friction" increases slightly with an increase in density.
3. The "cohesion" increases with an increase in moisture content to a peak value near the plastic limit, and then drops off rapidly.
4. At constant moisture content the "cohesion" increases with an increase in density.

TABLE 2.1

SUMMARY OF DIRECT SHEAR TEST RESULTS

(1) Test Number	(2) Moisture Content w % dry wt.	(3) Dry Density lbs./cu.ft.	(4) Angle of Friction ϕ degrees	(5) Cohesion Kips/sq.ft.
DS-1-1	10.3	98.4	33	0.57
DS-1-2	11.5	103.1	29	0.75
DS-1-3	14.5	107.5	28	1.15
DS-1-4	18.0	112.8	22	1.40
DS-2-1	17.40	95.2	23.5	1.00
DS-2-2	17.05	100.5	25.7	1.10
DS-2-3	17.00	110.5	26.6	1.57
DS-2-4	17.15	105.0	26.1	1.45

On Fig. 2.1 a curve has been plotted representing the shearing strength at various moisture contents of the soil, based on a normal load of 2 Kips per square foot (13.9 p.s.i.). It is of interest to note that the shearing resistance of the soil increases rapidly between 15% and 17% moisture content. The maximum strength is reached at the higher of these two values, which is near the plastic limit and is the same as that at which the maximum "cohesion" is developed. The pressure of 13.9 pounds per square inch is about equal to the unit dead weight plus dynamic force (without magnification) used in some of the tests with the Lazon oscillator in the pit. If the normal load is increased to 100 pounds per square inch, comparable to pressures attained in the pit at resonance, there is a decrease in total shearing resistance with increasing moisture content. As pointed out in Chapter 1, the shearing resistance of the compacted soil was only exceeded in the pit tests when the oscillator was operating at resonance.

2.3 Tests for Modulus of Elasticity in Shear

2.3.1 General

The Modulus of Elasticity in Shear, (Modulus of Rigidity), was determined because of its value in the general theory of vibration and wave propagation.

The Shearing Modulus of Elasticity of sand had previously been successfully determined by torsion of a column of the sand confined in a thin brass tube.^{(1)*} This same technique was tried with the Reseda CL soil, but the effect of the brass cylinder relative to that of the soil was so great that the accuracy was poor and the method was abandoned. Tests were successfully made by a similar technique using the compacted soil cylinder without the enclosing brass container

2.3.2 Apparatus

The apparatus for these tests is shown schematically in Fig. 2.2. The brass loading piston (1) provides a means of applying both longitudinal pressure and torque to the soil cylinder (5). The longitudinal load was applied by a Universal Testing Machine, and the torque by means of weights acting through wires over pulleys (2) and connected to the torque arms of the top loading piston. Slippage between the loading piston and the soil was minimized by glueing rough sandpaper to the brass plates.

In the first tests the angle of twist was obtained from the displacement of a dial gage (4), reading directly to 0.0001 inch, acting at a known distance from the center of the cylinder. This method lacked the accuracy and consistency desired, and in later tests the angular displacement was measured by optical means. In this technique the angle of twist was indicated by the relative rotation of two mirrors fixed to the sides of the soil column. Two lines of sight from fixed transits reflected from the mirrors to a target board on which the change in the position of the line of sight with twisting could be measured. This method was more sensitive than the use of dial gages, and reduced the possibility of disturbance from end effects and slipping

* The numbers in parentheses in superscribed position refer to the list of references at the end of this chapter.

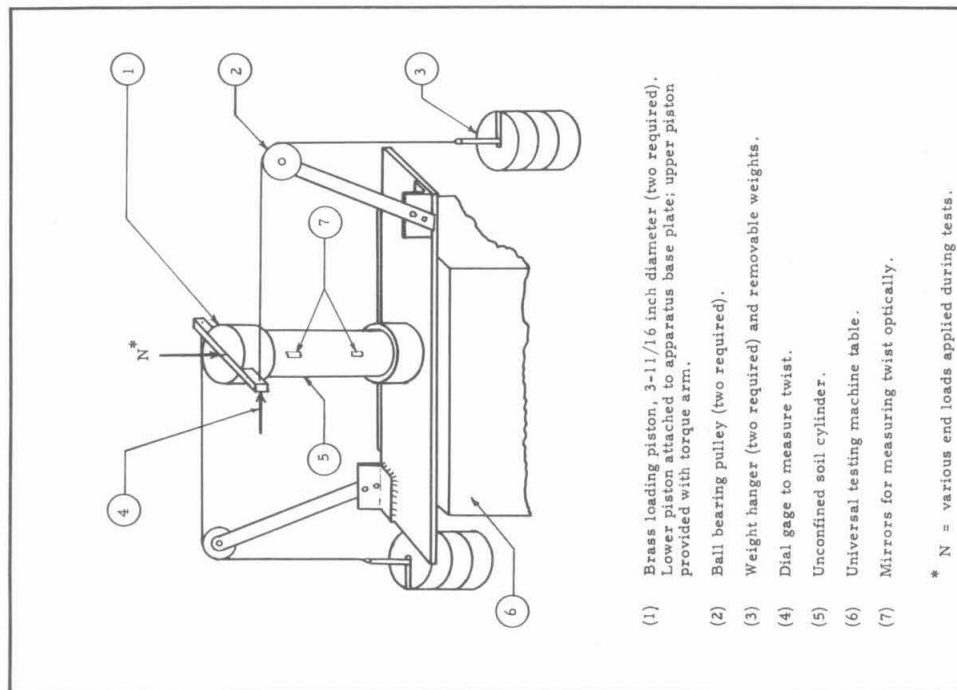


Fig. 2.2 APPARATUS USED IN THE EXPERIMENTAL DETERMINATION OF THE SHEARING MODULUS OF ELASTICITY OF RESEDA CL SOIL

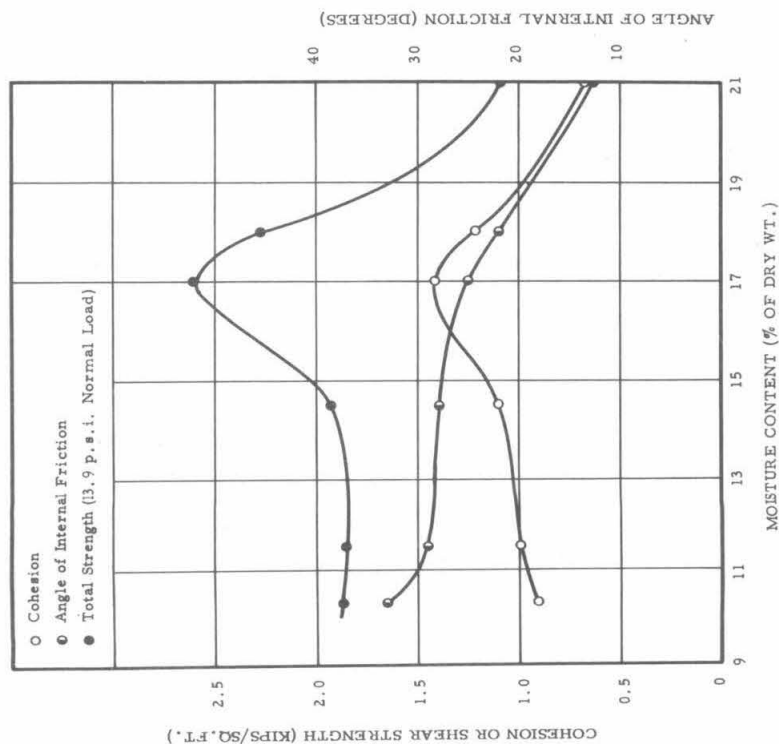


Fig. 2.1 RELATIONSHIP BETWEEN MOISTURE CONTENT AND COHESION, ANGLE OF INTERNAL FRICTION, AND SHEAR STRENGTH OF RESEDA CL SOIL

between the pistons and the soil.

2.3.3 Procedure

A soil sample at the desired moisture content was compacted into a cylinder 2.86 inches in diameter and about 10 inches long. Load was applied in a longitudinal direction and held until compression of the soil ceased. Torque was applied by adding small increments of weight simultaneously to the two loading pans to give torque values of 28, 56, and 84 pound inches. The angular deformation readings were taken two minutes after each increment of torque was applied. This interval was used because the major portion of the torsional flow appeared to have taken place within that time. This also agreed with the results of Geuze and Tjong-Kie,⁽²⁾ who found that in their tests with clay cylinders the largest part of the deformation took place immediately after the application of the load. After this the rate of angular creep approached a straight line. The values of G determined by the short time tests are considered more nearly correct for use with vibration compaction than those using the ultimate long time twist values.

Cylinders of soil were prepared at moisture contents varying from 10% to 21%, and at dry densities varying from 100 pounds per cubic foot to 125 pounds per cubic foot. The most dense cylinders were prepared by the standard compaction method used by the California State Highway Department. These specimens were easy to handle because of their strength and rigidity. When compacted at the lower densities comparable to between 90 and 95% of the maximum density given by the modified A.A.S.H.O. method, considerable difficulty was experienced in handling and testing because of the relative weakness of the cylinders.

2.3.4 Test Results

The summary of data and results is given in Table 2.2. Curves showing the relationship of Modulus of Elasticity in Shear to moisture content at various longitudinal compression values, for all samples compacted by the full California compaction method, are shown on Fig. 2.3.

The Shearing Modulus of Elasticity at the lower dry densities (106 to 116 lb./cu.ft.) comparable to ordinary compacted fills, and at moisture contents of from

TABLE 2.2

SUMMARY OF RESULTS FROM TORSION TESTS ON UNCONFINED CYLINDERS

Soil - Type CL from Reseda							
(1) Test No.	(2) Moisture Content	(3) Longitu- dinal Load	(4) Maximum Torque	(5) Number of Torque Increments	(6) Wet Density	(7) Dry Density	(8) Average Shearing Modulus of Elasticity G
	w % dry wt.	N lbs.	T* lb.-in.	M**	lb./cu.ft.	lb./cu.ft.	p.s.i
TU-1-1	16	150	72	2	133	114	259
TU-2-1	13.3	300	143	2	140	124	1200
TU-3-1	14.4	250	120	3	140	123	598
TU-4-1	15.0	150	72	2	138.5	120	294
TU-4-2	15.0	250	120	3	138.5	120	481
TU-4-3	15.0	350	167	2	138.5	120	836
TU-5-1	12.8	250	120	3	141.5	125	1037
TU-5-2	12.8	350	167	3	141.5	125	2330
TU-5-3	12.8	450	214	3	141.5	125	3550
TU-6-1	21.0	130	62	1	128.5	106	74
TU-7-1	13.4	350	167	3	141.5	125	1621
TU-7-2	13.4	450	214	3	141.5	125	2523
TU-7-3	13.4	450	214	3	141.5	125	2447
TU-8-1	12.1	250	120	3	137.3	119.5	1380
TU-8-2	9.6	250	120	3	132	119.5	4160
TU-9-1	16.3	250	120	3	135	116	204
TU-10-1	14.0	250	120	3	124	109	168
TU-11-1	13.7	250	120	2	120	106	159
TU-12-1	21.8	250	120	Failed	129.5	106	-

Notes: * Maximum allowable torque to prevent slipping between brass end pistons and soil sample.

** One increment equals 28 pound-inches of torque.

$$G = \frac{M \cdot L}{I \cdot \phi}$$

where M = applied torque,
 I = polar moment of inertia of cylinder,
 L = length of cylinder,
 ϕ = angle of twist (radians) in length L.

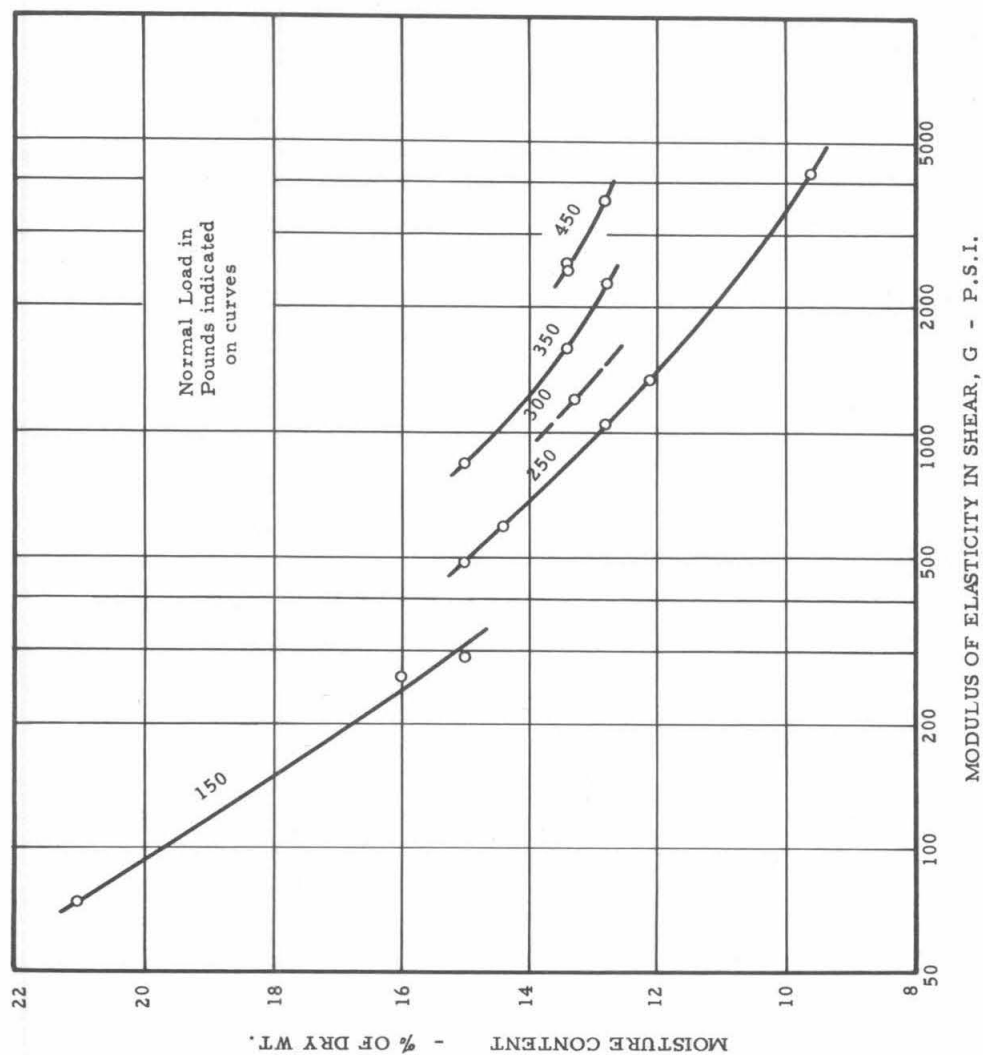
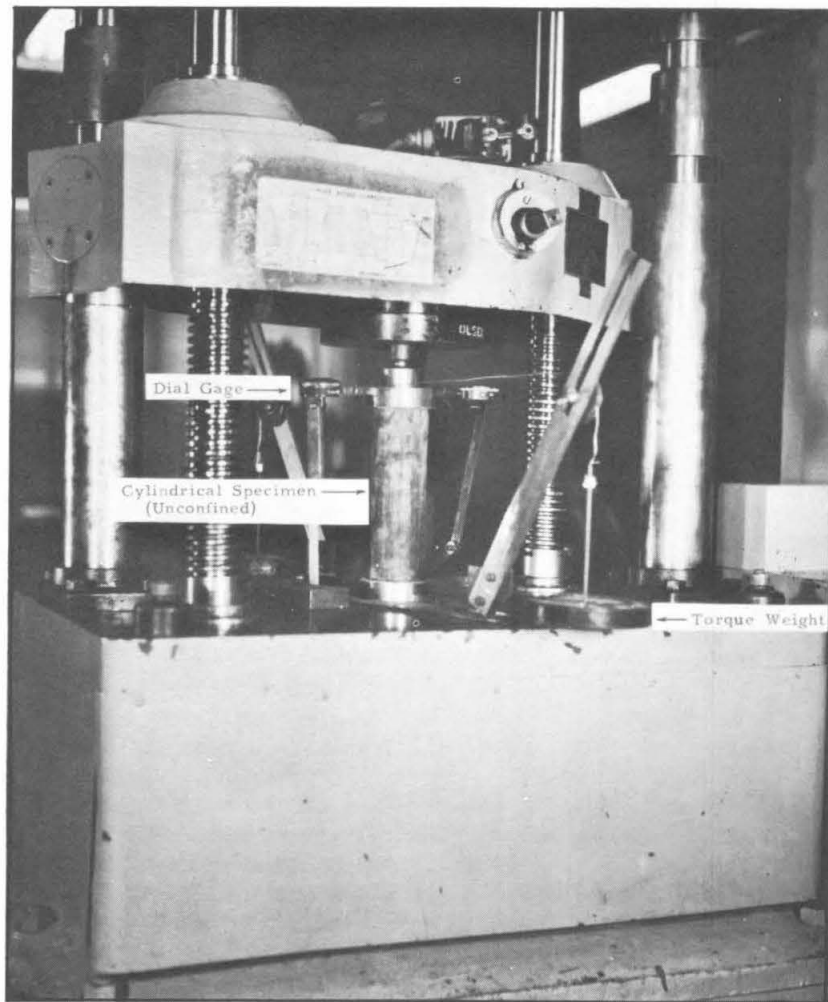
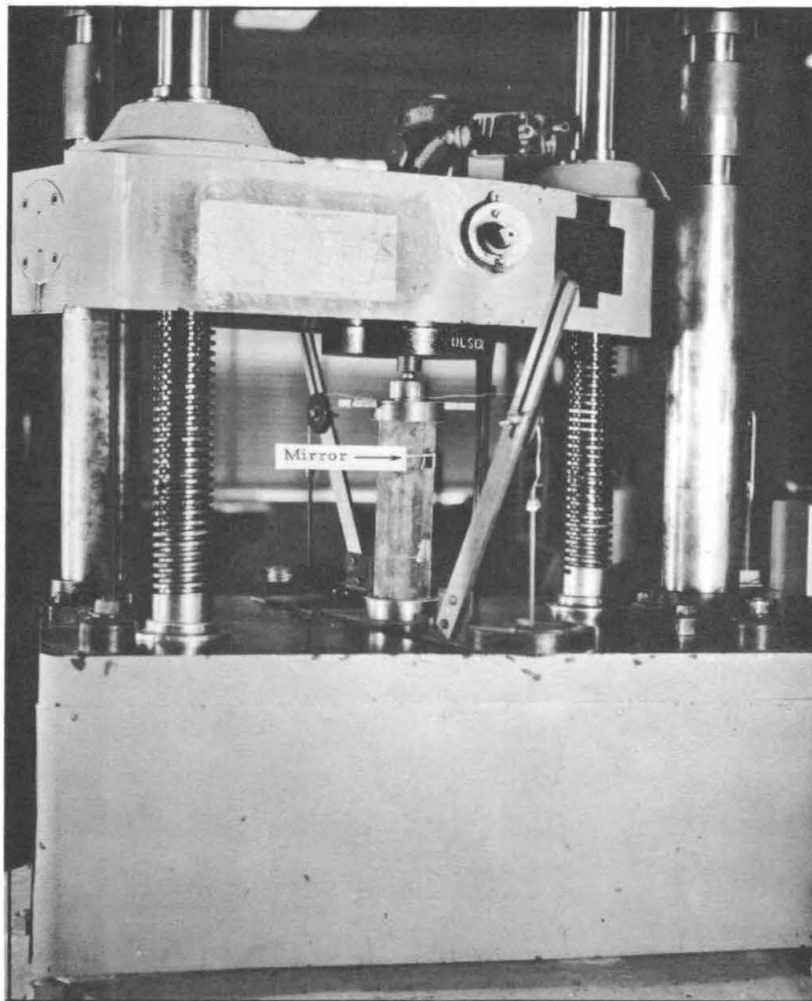


Fig. 2.3 RELATIONSHIP BETWEEN MOISTURE CONTENT AND
SHEARING MODULUS OF ELASTICITY OF RESEDA CL SOIL,
SHOWING EFFECT OF VARYING THE NORMAL LOAD.



(A) Apparatus for the Determination of the Shearing Modulus of Elasticity of Reseda CL Soil, using Dial Gages to Measure Angle of Twist.



(B) Apparatus for the Determination of the Shearing Modulus of Elasticity of Reseda CL Soil, using Optical Methods to Measure Angle of Twist.

13.7% to 16.3%, ranged from 159 to 204 pounds per square inch, under a longitudinal compression of 250 pounds per square inch.

At the higher dry densities (119.5 to 125 lb./cu.ft.) values of the Shearing Modulus reached a maximum of 4160 pounds per square inch. The high values are due not only to the effect of density but also to the effect of moisture content. Decreasing the moisture content produces an increase in the rigidity of the cylinder, and therefore an increase in the Modulus. This is specifically illustrated in specimen TU-8, which was first tested at 12.1% moisture under a longitudinal compression of 250 pounds per square inch, and then dried to 9.6% moisture and retested under the same compression load. The Shearing Modulus increased from 1380 pounds per square inch to 4160 pounds per square inch. This same effect has been noted in tests on concrete cylinders.⁽³⁾

The curves on Fig. 2.3 are of particular interest because they indicate an increasing Modulus with increasing longitudinal compression on the cylinder. Each curve at a given longitudinal compression shows a decrease in modulus with increasing moisture, and the curves at different values of longitudinal compression are parallel. The explanation for the increase in Modulus with increase in compression load is not clear. It cannot be accounted for by considering the increases in density nor the change in dimensions of the cylinder. The compression of the moisture films surrounding the soil particles may be partially responsible, but this does not appear to be a major effect because of the very small total compression (0.007 inches or less) that occurred in the cylinder when the axial load was applied. End effects on stress distribution and possible yielding between the end pistons and the soil were eliminated, or at least reduced to a large extent, by the optical technique in which the mirrors were attached at the quarter points of the cylinder length. Time was not available to investigate this phenomenon to its conclusion, and it is therefore recorded as an unexplained effect.

2.3.5 Conclusions

(1) The Modulus of Elasticity in shear for the cylinders compacted by the standard compaction method of the California State Highway Department varied from 481 pounds per square inch at a moisture content of 15.0% to 4160 pounds per square inch at a moisture content of 9.6%, for a longitudinal compression of 39 pounds per square inch and for dry densities between 119.5 and 125 pounds per cubic foot.

(2) For densities comparable to those used in the field tests, the Shearing Modulus of Elasticity varied from 159 pounds per square inch at 13.7% moisture content and a dry weight of 106 pounds per cubic foot, to 259 pounds per square inch at 16% moisture content and 114 pounds per cubic foot.

(3) There is a rapid increase in Shearing Modulus with decrease in soil moisture content.

(4) The Shearing Modulus of the cylindrical specimens increased with increase in longitudinal compression, other factors remaining constant.

REFERENCES

- (1) See reference (1), Chapter 1, p. 60 of this report.
- (2) Geuze, E. C. W. A., and Tjong-Kie, Tan: "Rheological Properties of Clays," Proceedings of Third International Conference on Soil Mechanics and Foundation Engineering, Zurich, 1953.
- (3) Pickett, G.: "Equations for Computing Elastic Constants from Flexural and Torsional Resonant Frequencies of Vibration of Prisms and Cylinders," Proceedings A.S.T.M., vol. 45, 1945.

CHAPTER 3

SUMMARY AND CONCLUSIONS

3.1 Discussion and Summary

In the previously submitted report--"Vibration Compaction of Cohesive Soils," December 1954--a number of tentative conclusions were presented. They were considered tentative because of the limited number of tests upon which they were based. Nevertheless it was clear that adequate compaction of the moderately cohesive soil, sandy loam, then being tested was possible if the conditions specified in the conclusions were met.

When research was undertaken on the much more cohesive soil used in the tests described in this report, the same general conditions for compaction were incorporated in the program. In the early stages of this program the same values of the parameters that had proved successful with the sandy loam were tried, but there was no effective compaction. Attention was then given to the two variables that appeared to warrant the closest investigation, namely the soil moisture content and the surface contact pressure. Investigation of the former provided few difficulties; the latter provided many, and was characterized by continuous frustration of efforts to obtain specified test conditions. In spite of this, the investigations of all of the parameters, as listed in Chapter 1, have provided much useful data from which a number of specific and tentative conclusions may be drawn.

The specific conclusions are not presented here, as they represent unique conditions that have no part in the general scheme of compaction by vibration. Thus there is no value in the conclusion that the optimum content for the adequate vibration compaction of Reseda CL soil is 20.6%. This only concerns a particular soil under the specific conditions of : (a) a vibrator of 1180 pounds dead weight operating at resonance; (b) a dynamic force of about seven-tenths of the dead weight; and (c) a base-plate 13-3/4 inches in diameter.

The tentative conclusions are of much greater importance, principally because they substantiate the conclusions, tentative or otherwise, drawn from the results of all previous work in this field at the California Institute of Technology. These conclusions are clearly defined within the limits of the tests so far performed, and the results appear to agree with the general concepts of shear failure and the development of plasticity beneath a loaded plate. However, the assumption that the stress distribution is the same for dynamic action as it is for static loading has not been proved. Nor has the effect of alternating stress and impulsive loading been determined. Until such effects are clearly established and correlated with a full range of test data, the conclusions must remain tentative.

A very general summary of the situation is that the results of all the work to date point in the same direction. Tentative conclusions derived from tests on one soil are substantiated when other types of soil are considered but few precise conclusions can be made. Certain regular trends or patterns in the relationships involving the various parameters are noticeable, but insufficient data are available to correlate these trends or patterns with the existing theory, or to derive empirical formulas in terms of basic soil properties.

3.2 Conclusions

From the experience with the three types of soil studied under this contract and its extensions, the following general conclusions may be drawn:

- (1) Satisfactory compaction of soils by vibration compaction is possible, even if the soils are of the fine-grained, cohesive type.
- (2) Vibration at the resonant frequency of the vibrator-soil system is of major importance in obtaining rapid and adequate consolidation.
- (3) A ratio of applied dynamic force to vibrator dead weight approximately equal to unity is desirable for maximum effectiveness.
- (4) The unit contact pressure, between the vibrator base and the soil surface, required to give adequate densities, increases as the soils become more cohesive.
 - (a) For dry cohesionless sand, only very low unit soil pressures are required. A value as low as 3 pounds per square inch gave excellent results.

(b) For the sandy loam soils tested, pressures of 4 pounds per square inch were used successfully.

(c) For the clay loam (CL) soil, pressures of 8 pounds per square inch were required.

The above values are the dead weight contact pressures only.

(5) There exists a moisture-density relationship of the same form as that found using orthodox laboratory and field compaction methods. The optimum moisture content was found to increase as the soils became more cohesive.

(a) For the sand tested, very satisfactory densities were obtained at a moisture content of about 3%. The optimum moisture content according to the modified A.A.S.H.O. method was 13%. In the vibration tests, increasing the moisture contents up to about 8% was found to develop cohesion, requiring an increased unit contact pressure to attain equal density.

(b) For the sandy loam soils, the optimum moisture content in these vibration tests was slightly in excess of the modified A.A.S.H.O. optimum.

(c) For the clay loam soil, the vibration optimum was considerably higher than the modified A.A.S.H.O. optimum, and slightly higher than the optimum given by the A.S.T.M. Standard Compact Test (D698-42T).

(6) The addition of certain chemicals to the soil tends to reduce the cohesion and therefore the effort necessary to compact the soil. For the sandy loams tested, Sodium Sulphate and Daxad 23 (a commercial dispersing agent) were particularly useful.

3.3 Recommendations for Future Studies

Any further investigations will require a vibrator capable of producing greater dynamic forces, at lower frequencies, than have been possible with the equipment available to date. It is suggested that the specifications for such a machine should show minimum requirements of a dynamic force of 5000 pounds at a frequency of 5 cycles per second; base-plates varying from one to three square feet in area; and a means of externally controlling the dynamic force at a given frequency as provided, for example, in the Lazan oscillator.

It is recommended that further studies be made to fully substantiate and prove, or otherwise, the conclusions and relationships established at the present time. In this respect, the following variables are considered of prime importance:

- (1) The moisture content of the soil.
- (2) The ratio of F_0/W .
- (3) The contact pressure between the base-plate and the soil surface.

To investigate the last variable, and to extend the knowledge of the basic physic . processes involved in the vibration-compaction of soils, the following items are suggested for consideration:

- (1) Direct measurement of contact pressures.
- (2) Measurement of the distribution of pressures within the soil mass.
- (3) Measurement of the amount and direction of movement of the soil during vibration.

Aspects of less importance to the basic work, but nevertheless greatly effecting the translation of this work into practical use are:

- (1) The question of movement of the vibrator over the soil surface, and the number of passes required to obtain satisfactory densities.
- (2) The use of rollers instead of flat plates to support the vibrator.
- (3) The confinement of the soil surface by a material of greater stiffness, such as asphalt or asphaltic-concrete.
- (4) The use of dynamic forces generated by a single rotating force vector.

Future studies as recommended above should include attempts to correlate test data with a suitable theory, or the establishment of empirical relationships based on these data.

